PLOS | GENETICS

RESEARCH ARTICLE

Evolution and multiple roles of the Pancrustacea specific transcription factor *zelda* in insects

Lupis Ribeiro[1,2], Vitória Tobias-Santos[1], Daniele Santos[1], Felipe Antunes[1], Geórgia Feltran[1], Jackson de Souza Menezes[1], L. Aravind[3], Thiago M. Venancio[2]*, Rodrigo Nunes da Fonseca[1]*

1 Laboratório Integrado de Bioquímica Hatisaburo Masuda, Núcleo em Ecologia e Desenvolvimento SócioAmbiental de Macaé (NUPEM), Campus UFRJ Macaé, Instituto Nacional de Ciência e Tecnologia em Entomologia Molecular - INCT-EM, Macaé, Brazil, **2** Laboratório de Química e Função de Proteínas e Peptídeos, Centro de Biociências e Biotecnologia, Universidade Estadual do Norte Fluminense Darcy Ribeiro, Instituto Nacional de Ciência e Tecnologia em Entomologia Molecular - INCT-EM, Rio de Janeiro, Brazil, **3** National Center for Biotechnology Information, National Library of Medicine, National Institutes of Health, Bethesda, Maryland, United States of America

* thiago.venancio@gmail.com (TMV); rodrigo.nunes.da.fonseca@gmail.com (RNdF)

Citation: Ribeiro L, Tobias-Santos V, Santos D, Antunes F, Feltran G, de Souza Menezes J, et al. (2017) Evolution and multiple roles of the Pancrustacea specific transcription factor *zelda* in insects. PLoS Genet 13(7): e1006868. https://doi.org/10.1371/journal.pgen.1006868

Editor: Claude Desplan, New York University, UNITED STATES

Received: April 17, 2017

Accepted: June 14, 2017

Published: July 3, 2017

Data Availability Statement: All relevant data are within the paper and its Supporting Information files.

Funding: This work was supported by: NIH Intramural Funding to LA; FAPERJ/RJ/BRAZIL to TMV and RNdF www.faperj.br; and CNPq/BRAZIL to TMV and RNdF www.cnpq.br. The funders had no role in study design, data collection and analysis, decision to publish, or preparation of the manuscript.

Abstract

Gene regulatory networks (GRNs) evolve as a result of the coevolutionary processes acting on transcription factors (TFs) and the cis-regulatory modules they bind. The zinc-finger TF *zelda (zld)* is essential for the maternal-to-zygotic transition (MZT) in *Drosophila melanogaster*, where it directly binds over thousand cis-regulatory modules to regulate chromatin accessibility. *D. melanogaster* displays a long germ type of embryonic development, where all segments are simultaneously generated along the whole egg. However, it remains unclear if *zld* is also involved in the MZT of short-germ insects (including those from basal lineages) or in other biological processes. Here we show that *zld* is an innovation of the Pancrustacea lineage, being absent in more distant arthropods (e.g. chelicerates) and other organisms. To better understand *zld´s* ancestral function, we thoroughly investigated its roles in a short-germ beetle, *Tribolium castaneum*, using molecular biology and computational approaches. Our results demonstrate roles for *zld* not only during the MZT, but also in posterior segmentation and patterning of imaginal disc derived structures. Further, we also demonstrate that *zld* is critical for posterior segmentation in the hemipteran *Rhodnius prolixus*, indicating this function predates the origin of holometabolous insects and was subsequently lost in long-germ insects. Our results unveil new roles of *zld* in different biological contexts and suggest that changes in expression of *zld* (and probably other major TFs) are critical in the evolution of insect GRNs.

Author summary

Pioneer transcription factors (TFs) are considered the first regulators of chromatin accessibility in fruit flies and vertebrates, modulating the expression of a large number of target

Competing interests: The authors have declared that no competing interests exist.

genes. In fruit flies, *zelda* resembles a pioneer TF, being essential during early embryogenesis. However, the evolutionary origins and ancestral functions of *zelda* remain largely unknown. Through a number of gene silencing, microscopy and evolutionary analysis, the present work shows that *zelda* is an innovation of the Pancrustacea lineage, governing not only the MZT in the short-germ insect *Tribolium castaneum*, but also posterior segmentation and post-embryonic patterning of imaginal disc derived structures such as wings, legs and antennae. Further, *zelda* regulation of posterior segmentation predates the origin of insects with complete metamorphosis (holometabolous), as supported by gene silencing experiments in the kissing bug *Rhodnius prolixus*. We hypothesize that the emergence of *zelda* contributed to the evolution of gene regulatory networks and new morphological structures of insects.

Introduction

Gene regulatory networks (GRNs) depend on the coevolution of transcription factors (TFs) and their relationship with the cis-regulatory modules (CRMs) they bind [1, 2]. In insects, the detailed role of a number of TFs and CRMs have been well-described, particularly during the embryogenesis of the fruit fly *Drosophila melanogaster* [3].

In metazoans, the period following fertilization is typically characterized by rapid and near-synchronous mitotic divisions and cleavages that occur under conditions of minimal cellular differentiation. Cleavages typically depend on maternally supplied factors and zygotic genome transcription is constrained during this early period of development [4]. A conserved process of metazoan embryogenesis is the maternal-to-zygotic transition (MZT), which is characterized by two critical steps: 1) the elimination of a maternal set of mRNAs and proteins and; 2) the beginning of zygotic transcription, which leads to the zygotic genomic control of development [5]. In *D. melanogaster*, the majority of the first set of zygotic transcripts are regulated by *zelda (zld)* [6], a zinc finger TF with particular affinity for promoter regions containing TAG-team sites—heptamers constituted by CAGGTAG and its variants [7–9]. *zld* (*Dm-zld*, in *D. melanogaster*) binding sites have been identified in *D. melanogaster* embryos (cycles 8 to 14) by chromatin immunoprecipitation coupled with high-throughput sequencing (ChIP-Seq) [8]. *Dm-zld* regulates a large set of genes involved in important processes such as cytoskeleton organization, cellularization, germ band development, pattern formation, sex determination and miRNA biogenesis [6]. *Dm-zld* was also suggested to participate in larval wing disc development [10] and its overexpression during wing imaginal disc formation led to wing blisters in adults, an indicative of improper adherence of ventral and dorsal wing epithelia [11]. Nevertheless, while *zld´s* functions have been thoroughly investigated in *D. melanogaster* MZT, its roles in other organisms and biological processes remain elusive.

D. melanogaster displays a long germ type of embryonic development, during which all segments are simultaneously generated along the whole egg. In contrast, short germ insects generate anterior (e.g. head) segments early in development, while the remaining segments are patterned from the posterior region, the growth zone (GZ). Since short germ development is considered to be the ancestral mode of development, short-germ insects have been established as developmental model systems [12, 13]. The short-germ red flour beetle *Tribolium castaneum* (*Tc*) was the first beetle species to have its genome completely sequenced [14]. *T. castaneum* displays a short life-cycle and is amenable to gene silencing via RNAi [15], gene overexpression [16], specific tissue expression [17] and fluorescence labeling during early development [18]. Several developmental processes that have been investigated in *T.*

castaneum were lost or extensively modified in the *D. melanogaster* lineage, such as GZ formation [19], extensive extra-embryonic morphogenesis [20] and the formation of a morphologically complex head during embryogenesis [21]. Early development of *T. castaneum* is similar to most other insect groups, in which synchronous rounds of division are followed by nuclear migration to the egg cortex and cellularization, forming the so called uniform blastoderm [18, 22]. Taken together, all the genetic and morphological information on *T. castaneum* early development, along with the established techniques mentioned above, make this beetle an ideal model to understand the evolution of *zld´s* function during insect development.

In the present work, we provide the first comprehensive analysis of *zld* orthologs across a wide range of species. Further, we provide functional analysis of a *zld* ortholog in a non-Drosophillid insect, the short germ beetle *T. castaneum* (thenceforth referred as *Tc-zld*). Among our main results are: 1) The identification of some previously overlooked conserved domains in Zld; 2) An inference of the evolutionary origin of *Zld*, based on phyletic analysis in various hexapods and crustaceans; 3) The identification of a conserved set of 141 putative *Tc-zld* targets (i.e. genes with upstream TAGteam sequences), enriched in TFs, whose homologs that have been demonstrated to be *zld* targets in *D. melanogaster*; 4) Identification of key roles played by *Tc-zld* during the MZT; 5) Identification and experimental validation of two new biological roles of *zld* in *T. castaneum*: segment generation from the posterior GZ during embryogenesis and postembryonic imaginal disc development; 6) Demonstration that *zld* is also involved in GZ patterning in the hemipteran *Rhodnius prolixus*, supporting a conserved role in the GZ of a distant short-germ species. Altogether, our results unveil new roles of *zld* as a pleiotropic TF acting in various developmental processes across distantly-related insects.

Results/Discussion

Identification of conserved domains and tracing the origin of *zld*

While previous studies reported that *zld* is involved in the MZT of *D. melanogaster* [6], its evolutionary history remains unclear. We investigated the phyletic distribution of *zld* and found a single ortholog in all the inspected insect genomes, including the beetle *T. castaneum* (Fig 1; S1 Table), indicating that insects are sensitive to increased copy number of this important regulator, which is interesting considering that different TF families are particularly prone to expansions across insect lineages [23]. Further, *zld* homologs were also found in some (but not all) collembolan and crustacean genomes (Fig 1B; S1 Table). The canonical domain architecture of Zld has been reported as comprising a JAZ zinc finger (Pfam: zf-C2H2_JAZ) domain and a C-terminal cluster of four DNA binding C2H2 zinc finger domains (zf-C2H2) [6, 11, 24]. However, we performed a sensitive and detailed analysis of Zld proteins from multiple species and found other notable conserved protein domains and structural features. Firstly, we found two additional zf-C2H2 domains, N-terminal to the JAZ domain (Fig 1A). The most N-terminal zf-C2H2 is absent or partially eroded (i.e. without the conserved cysteines and histidines) in some species (Fig 1B), including *D. melanogaster*. We define this N-terminal zf as ZF-Novel, since it has not been reported in previous studies. This observation was confirmed by inspecting *Dm-zld* alternative splicing isoforms. On the other hand, the second N-terminal zf-C2H2 domain is conserved in virtually all extant insects, but absent or degenerate in the other Pancrustaceans (e.g. *Daphnia magna*; partially conserved, with one lost cysteine) (Fig 1). Further, between this second zf-C2H2 and the JAZ domain, there is a strikingly conserved acidic patch that is characterized by an absolutely conserved motif of the form [DE]I[LW]DLD (Fig 1), which is predicted to adopt an extended conformation (using the JPRED software [25]) amidst surrounding disordered regions. A related conserved acidic motif was also found in the chordate protein CECR2, C-terminal to the DDT and WHIM motifs, which constitute a helical

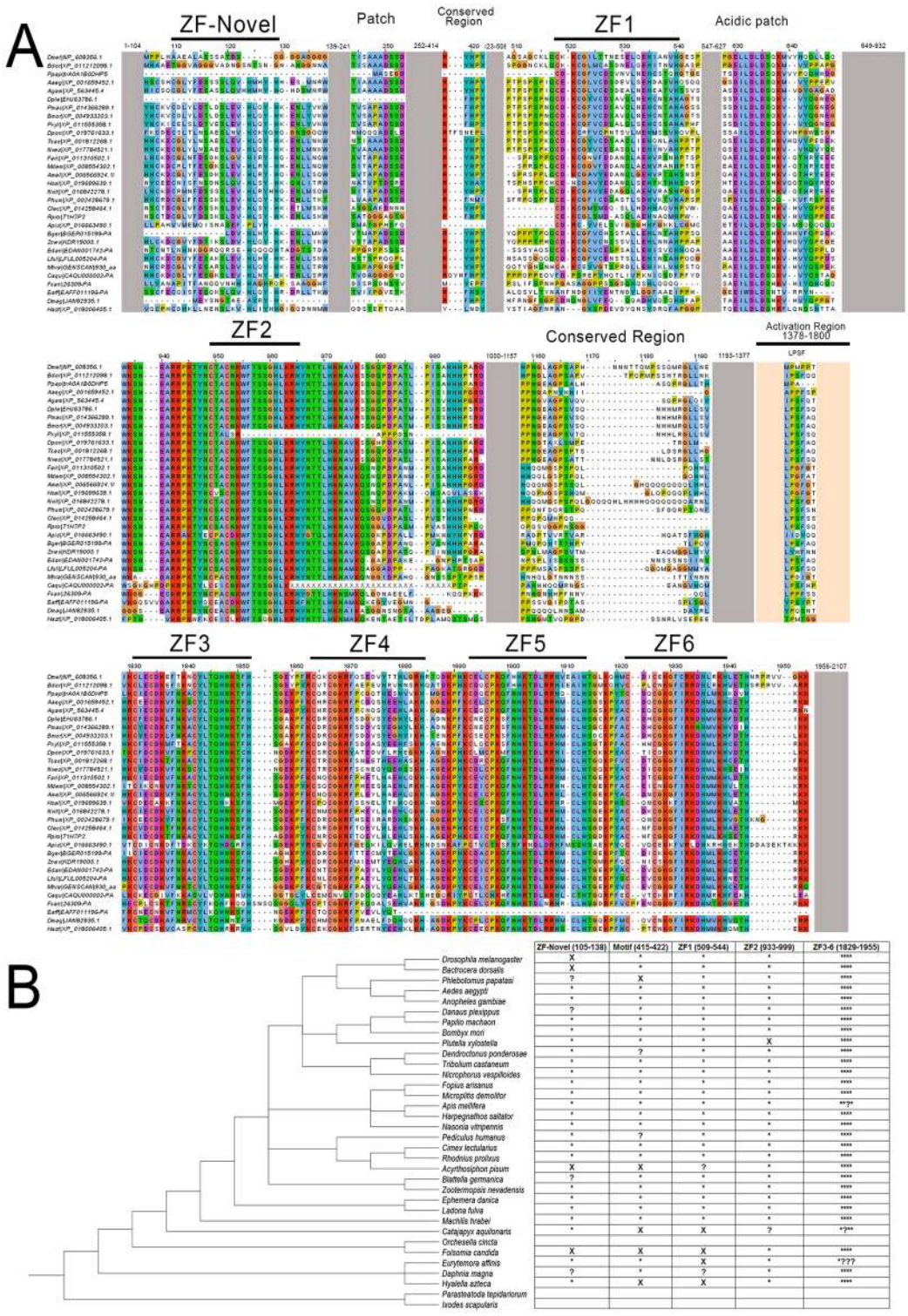

Fig 1. Tc-Zld proteins from insects and crustaceans. (A) Multiple sequence alignment of Zelda proteins, representing major groups of arthropods. (B) Conserved protein architecture features of Zelda proteins. Asterisks and x marks represent presence and absence, respectively. Question marks denote that the feature is either partially preserved or could be flagged as absent due to sequencing or assembly errors (e.g. wrong start codons). The cladogram was organized according to a previously reported phylogenetic study [79]. Two outgroups without *zld* orthologs were also included.

https://doi.org/10.1371/journal.pgen.1006868.g001

domain involved in setting the nucleosome spacing in conjunction with the ISWI ATPase during chromatin remodeling [26]. An analogous conserved acidic patch is also seen in the HUN domain which functions as a histones chaperone [27]. Taken together, these observations raise the possibility that this Zld acidic region interacts with positively charged chromatin proteins such as histones. A largely disordered region, between the JAZ finger and the cluster of 4 widely-conserved zf-C2H2 domains, has been shown to be important for *Dm-zld* transactivation *in vitro* [24]. Our analysis of evolutionary constraints on the protein sequence also revealed a motif of the form hP[IVM]SxHHHPxRD, which appears to be under selection for retention despite the strong divergence in this region. Hence, it is possible that it specifically plays a role in transactivation. Further, between the two N-terminal zf-C2H2 domains, there is a highly conserved RYHPY motif, which could be involved in nuclear localization (Fig 1A), as predicted for other TFs [28]. Given the conservation of these additional domains, we hypothesize that they also play important roles in Zld functions that were previously attributed exclusively to the C-terminal domains.

Aiming to elucidate the origins of *zld*, we performed extensive sequence searches and were unable to find homologs with the conserved canonical domain architecture outside of Pancrustacea, indicating that *zld* is an innovation of this lineage. We detected clear *zld* homologs across insects, including the termite *Zootermopsis nevadensis* (Order Isoptera), the scarce chaser *Ladona fulva* (Order Odonata), the mayfly *Ephemera danica* (Order Ephemeroptera) and *Machilis hrabei* (Order Archaeognatha). *zld* homologs were also found in crustaceans belonging to different classes (*Daphnia magna*, *Hyalella azteca* and *Eurytemora affinis*), as well as in the collembola *Folsomia candida*. Curiously, we found no *zld* in the genome of *Orchesella cincta* (collembola) and *Daphnia pulex* (crustacean), suggesting either that it is not absolutely conserved outside of insects or missing due to incompleteness of the deposited genomes. Specifically, we carefully searched the genomes of other non-insect arthropods, including chelicerates (e.g. the tick *Ixodes scapularis* and the spider *Parasteatoda tepidariorum*), and found no proteins with the canonical Zld domain organization (Fig 1B). General searches on Genbank against non-Pancrustacea arthropod proteins also returned no Zld orthologs. Although BLAST searches with Zld proteins against the *nr* and *refseq* databases recovered a number of significant hits in several distant eukaryotes, the similarity is almost always restricted to the C-terminal cluster of four Zf-C2H2 domains, which are very common across several TF families (e.g. *glass*, *earmuff/fez*, *senseless/gfi-1 and jim*). Taken together, our results support the early emergence of *zld* in the Pancrustacea lineage, with subsequent losses in particular species. Importantly, all the insect genomes we inspected have exactly one *zld* gene, indicating that this gene became essential in hexapods.

Tc-zld is a master regulator of signaling genes and other transcription factors

Previous studies in *D. melanogaster* using microarrays and ChIP-Seq revealed that *Dm-zld* regulates the transcription of hundreds of genes during early embryogenesis [6, 9, 29]. In *D. melanogaster*, enhancers bound by Dm-Zld are characterized by a consensus sequence CAGGTAG (i.e. TAGteam sequence), which is overrepresented in early zygotic activated genes, including TFs involved in AP and DV patterning [7, 8]. Since the TAGteam motif identified in *D. melanogaster* is conserved in *A. aegypti* [30], we investigated whether we could predict *Tc-zld* targets by detecting TAGteam motifs in the upstream regions of *T. castaneum* genes.

Firstly, an *ab initio* approach using DREME [31] was employed to analyze 2kb upstream regions of all *T. castaneum* protein-coding genes. This analysis uncovered a motif (i.e. GTAGGTAY) that is nearly identical to the TAGteam motif (Fig 2A). We used the *D.*

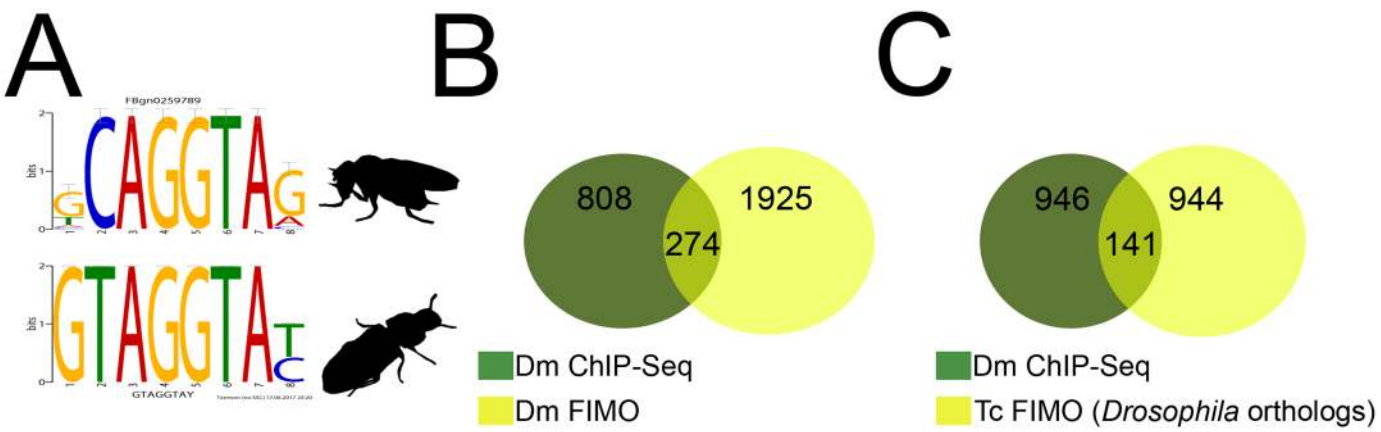

Fig 2. Computational identification of *Tc-zelda* target genes. (A) TOMTOM comparison of *D. melanogaster* motif similar to the TAGteam [7] obtained by DREME and putative *T. castaneum zld* DREME motif. (B) Venn diagram of the *D. melanogaster* ChIP-Seq MZT regulated genes (green) from [8] and *D. melanogaster* genes predicted by FIMO analysis with the putative DREME motif (yellow). (C) Venn diagram of the *D. melanogaster* Dm-Zld MZT targets (green) [8] and *D. melanogaster* one-to-one orthologs of putative *Tc-zld* targets.

https://doi.org/10.1371/journal.pgen.1006868.g002

melanogaster genome and experimental data [6, 9, 29] to validate our approach and found a significant overlap between experimental and predicted *zld* targets in *D. melanogaster* (Fig 2B). The putative *T. castaneum* motif was then used to screen the *T. castaneum* genome, resulting in the identification of 3,250 putative *zld* targets, representing ~19% of the *T. castaneum* genome (Fig 2C, S2 Table). Comparison of the putative *Tc-zld* targets with 1,087 genes regulated by Zld during *D. melanogaster* MZT [8, 29] allowed the identification of 141 *D. melanogaster* genes for which one-to-one orthologs figured among the putative *Tc-zld* targets (hypergeometric distribution, $P < 4.5\text{x}10^{-4}$; Fig 2C, S3 Table). Functional analysis of this gene set using DAVID [32] uncovered the enrichment of important categories, including a highly significant cluster of 26 homeobox TFs (S4 Table) and other significant clusters comprising genes involved in regionalization and segment specification, imaginal disc formation and metamorphosis (S4 Table). Interestingly, this gene set included multiple developmental regulators such as anteroposterior (AP), gap, pair-rule, homeotic and dorsoventral (DV) genes (S2 Table). Since several of these genes are involved in early developmental processes, we focused our initial analysis of *Tc-zld*'s function during embryogenesis.

Tc-zld is maternally provided and dynamically expressed during embryogenesis

Since *zld* is maternally expressed in the germ line in *D. melanogaster*, we compared its transcription in *T. castaneum* female ovaries and carcass by qRT-PCR. *T. castaneum* early development starts with synchronous divisions during the first three hours of embryogenesis (at 30˚C), followed by nuclear migration to the egg cortex and membrane segregation of nuclei into separate cells, approximately 7–8 hours after egg lay [18, 22]. We found that *Tc-zld* is highly expressed in the ovaries (Fig 3A), supporting the transcription of *Tc-zld* in the germ line. The abundance of *Tc-zld* transcripts is also higher in the first three hours of development than in the next two 3-hour periods (i.e. 3–6 and 6–9 hours) (Fig 3B), suggesting that *Tc-zld* mRNA is maternally provided and degraded after the first 3 hours of development. An antibody against the transcriptionally active form of RNA polymerase II, previously used in other ecdysozoan species [33, 34], showed that zygotic transcription in *T. castaneum* begins between three and six hours of development, shortly after the nuclei have reached the periphery (Fig 4).

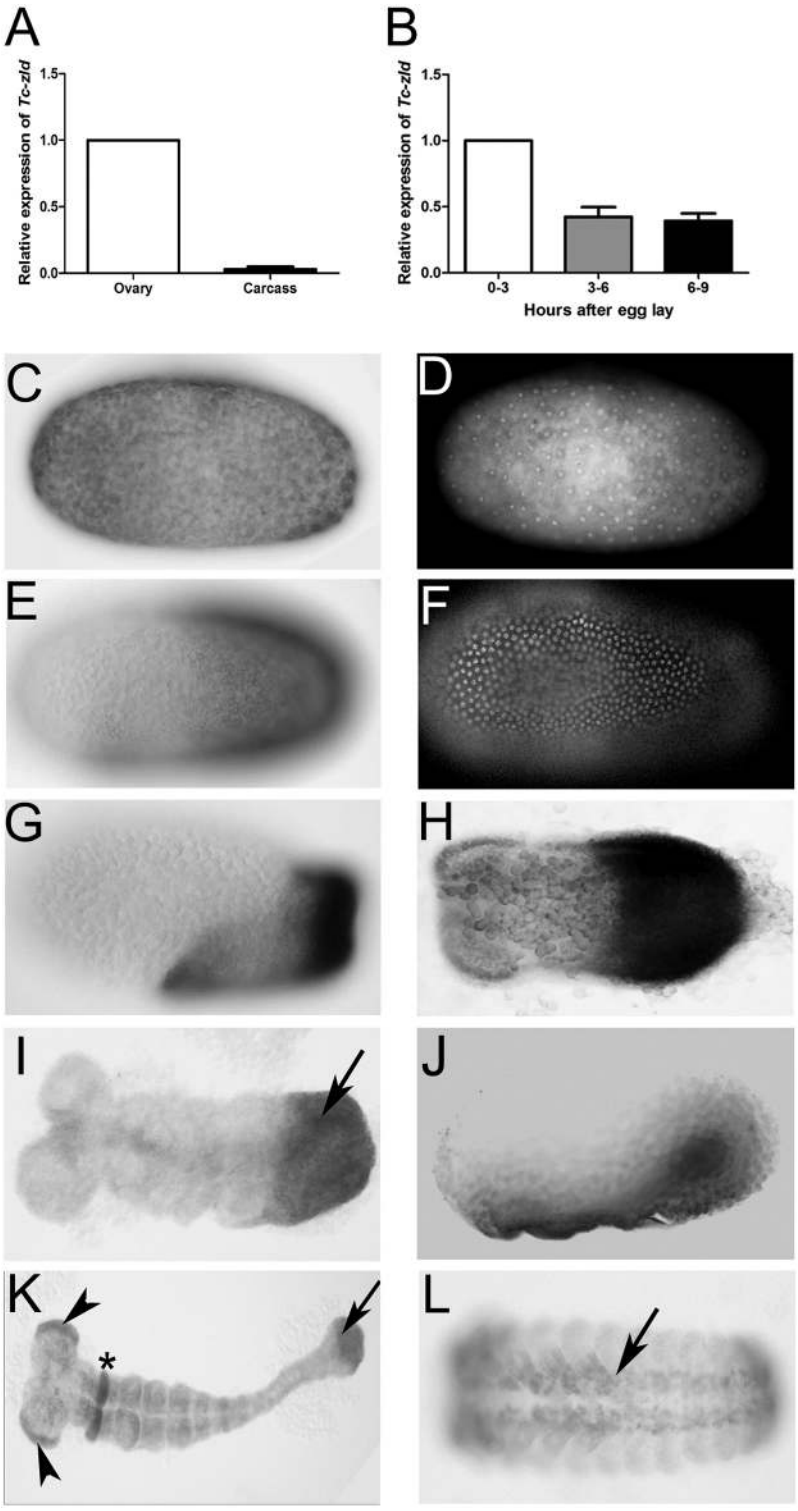

Fig 3. *Tc-zelda* is maternally provided and progressively confined to the posterior growth-zone during embryonic development. In all embryos, the anterior region points to the left. (A) Relative expression of *Tc-zld* in ovary and carcass. (B) Relative expression of *Tc-zld* 0–3, 3–6 and 6–9 hours after egg lay. Expression values were normalized using the constitutive gene *rps3* in both experiments. (C) Pre-blastoderm stage embryo (0–3 hours) shows *Tc-zld* transcripts uniformly distributed and its respective DAPI staining in D. (E) At uniform blastoderm stage (3–6 hours) transcripts begin to occupy the germ rudiment, respective DAPI

in F. (G) Shortly before posterior invagination, *zld* expression occurs along the whole germ rudiment, with higher levels at the posterior region where growth zone will form (6–9 hours). (H) Shortly before the beginning of germ band elongation *zld* expression is highly expressed at the GZ, although lower levels of mRNA can be observed at the along the whole embryonic region. (I) Approx. 13 hours after egg lay (AEL), during the beginning of germ band extension, *Tc-zld* is expressed at the posterior GZ (arrow). (J) An embryo slightly older than the one in H, highlighting *Tc-zld* expression at ventral serosal cells during serosal window closure. (K) Approx. 18-21hours AEL *zld* is still expressed at the posterior most region (arrow), head lobes (arrowheads) and a single gnathal segment (asterisk). (L) Approx. 39–48 hours AEL, during early dorsal closure, expression is observed at the nervous system (arrow).

https://doi.org/10.1371/journal.pgen.1006868.g003

In situ hybridization confirmed maternal ubiquitous expression of *Tc-zld* in the first three hours of development (Fig 3C and 3D) and showed a progressive confinement of *Tc-zld* mRNA to the posterior region of the egg, where the germ rudiment will be formed (Fig 3E and 3F). Between 6 and 9 hours of development, *Tc-zld* expression is observed at the embryonic tissue (Fig 3G), with higher levels at the posterior region (Fig 3H), where the GZ will generate new segments [19, 35]. In addition, *Tc-zld* is also expressed in the ventral serosa, during the serosal window closure (Fig 3J). Later in development, *Tc-zld* expression is still detected at the GZ (Fig 3I), at the head lobes and a single gnathal segment (Fig 3K) and, subsequently, in the nervous system (Fig 3L). Although *zld* is maternally provided, and zygotically expressed at the neural progenitors of both *D. melanogaster* and *T. castaneum* [6, 11], biased posterior expression is a feature so far described only in short-germ insects like the latter.

Parental injection of *Tc-zld* dsRNA reduces number of eggs laid and impairs embryogenesis

It has been shown that injection of dsRNA in *T. castaneum* females leads to reduced expression of a given gene in the females and their offspring, in a phenomenon called parental RNAi (pRNAi) effect [15]. We injected *zld* dsRNA in females and analyzed *Tc-zld* transcriptional levels during embryogenesis by qRT-PCR. After *zld* pRNAi, *Tc-zld* mRNA levels were reduced in the first two weeks of egg laying, severely impairing larval hatching (Fig 5A–5C). Importantly, identical knockdown phenotypes during embryogenesis were obtained by using a second,

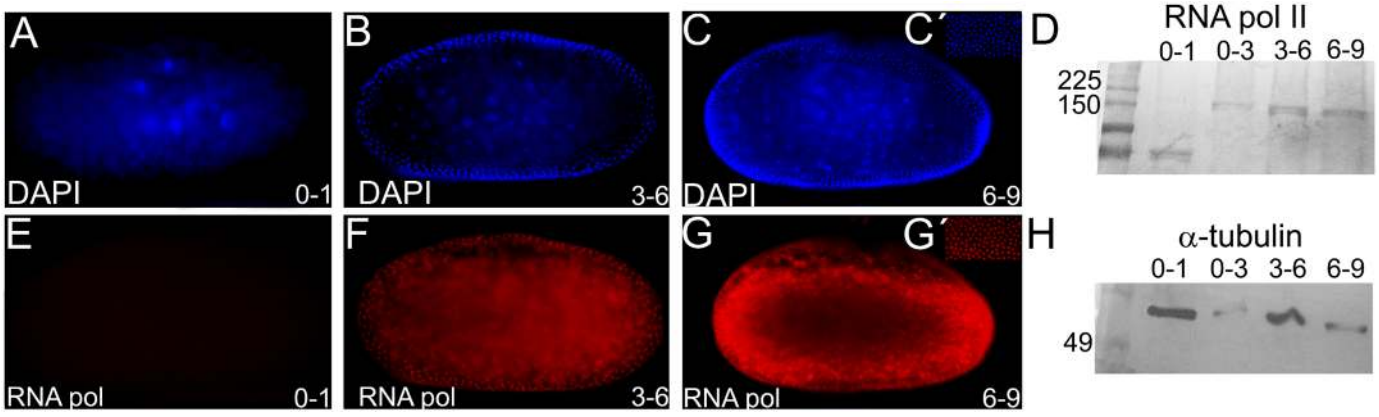

Fig 4. The onset of Maternal Zygotic Transition (MZT) in *Tribolium castaneum*. (A-C) Nuclear DAPI staining of *T. castaneum* embryos between 0–1 hours (A), 3–6 hours (B) and 6–9 hours after oviposition (C). (D,H) Western-blots of embryonic extracts from 0–1, 0–3, 3–6 and 6–9 hours after oviposition using an antibody against the transcriptionally active form of RNA pol II, as previously described [33]. (D) or an antibody against the α-tubulin protein as a loading control (H). (E,F,G) Immunostaining showing nuclear RNA pol II at 3–6 hours (F) and 6–9 hours (G), but not at 0–1 hour (E) after oviposition. Coupling RNA pol II staining with nuclear DAPI staining shows that *T. castaneum* zygotic transcription starts between 3–6 hours after egg laying, when the energids reaches the periphery (Fig 2A-C-DAPI and E-G-RNA pol II). Similar results were obtained by western-blots using the same antibody (D).

https://doi.org/10.1371/journal.pgen.1006868.g004

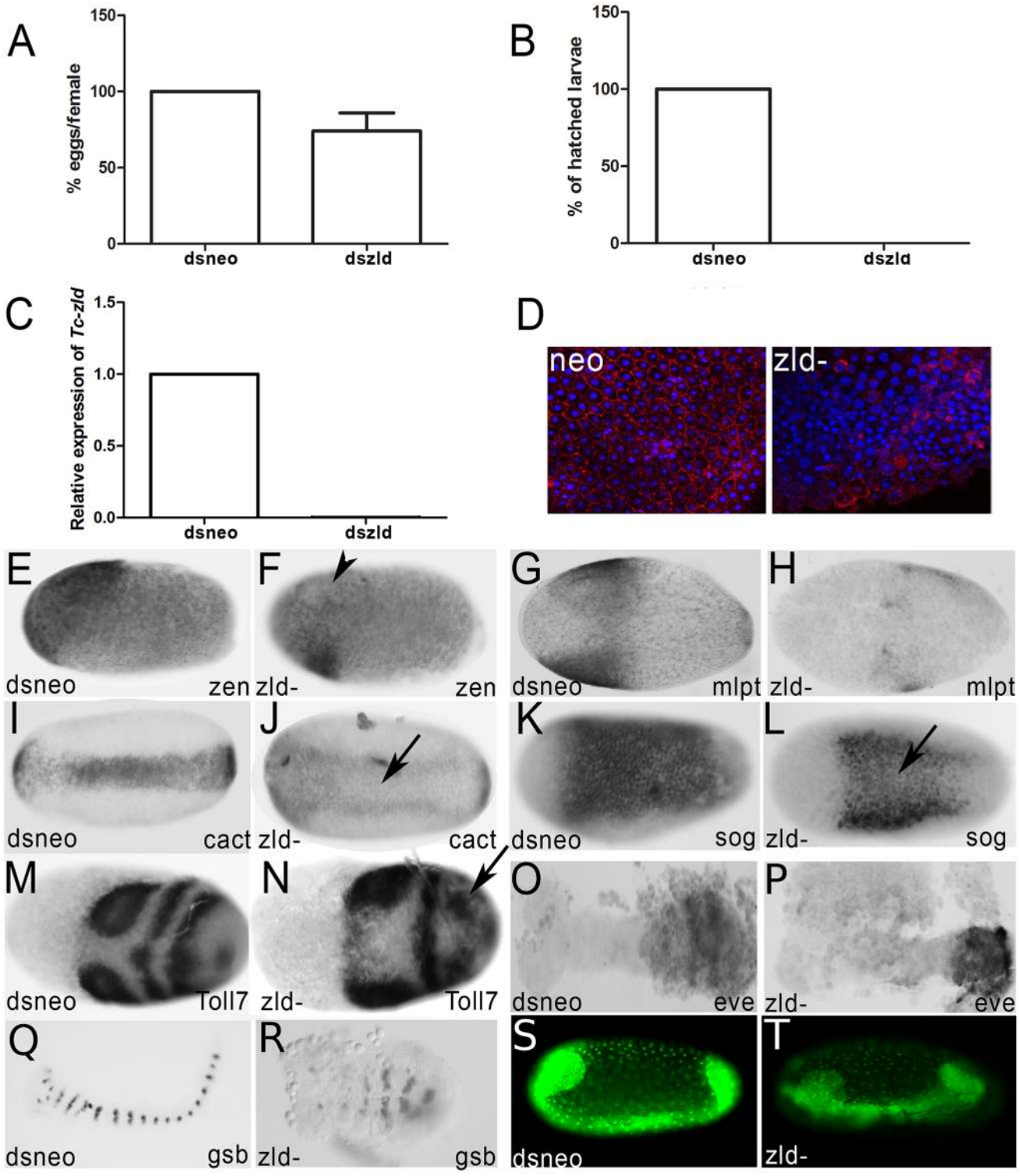

Fig 5. *Tc-zelda* parental RNAi affects oviposition and cellularization, while embryonic RNAi affects embryonic posterior patterning. (A) Normalized number of *dsneo* and *dszld* RNAi collected eggs. *zld* pRNAi reduces oviposition. (B) Percentage of hatched larvae obtained from eggs after *zld* pRNAi in comparison to the control (*dsneo* RNAi). *zld* pRNAi leads to lethality during embryogenesis. (C) Relative expression of *zld* in *dsneo* RNAi (control) and *dszld* RNAi during the first two egg lays. *zld* pRNAi almost completely abolishes *zld* expression. (D) Phospho-tyrosine (red) and DAPI (blue) staining in *dsneo* and *zld* RNAi eggs during cellularization. *zld* pRNAi impairs cellularization. (E,F) *Tc-zen* expression in the serosa [36] is reduced after *Tc-zld* pRNAi (arrowhead) when compared to the *dsneo* control. (G,H) Expression of the

gap gene *Tc-mlpt* [37] in control (G) and *zld* RNAi (H). *Tc-mlpt* loses its anterior expression domain in *zld* RNAi when compared to control. (I,J) The expression of the dorsoventral gene *Tc-cactus* [38] was reduced after *Tc-zld* pRNAi (J-arrow) when compared to the (I) control.(K,L) The expression of the dorsoventral gene *Tc-sog* was reduced after *Tc-zld* pRNAi (J-arrow) when compared to the (I) control. (M,N) Expression of *Tc-Toll7* was affected in the posterior region of *Tc-zld* RNAi embryos (N) when compared to *dsneo* (M). (O,P) Expression of the segmentation gene *Tc-eve* in control (O) and *zld* RNAi (P). *Tc-eve* expression is essential for segmentation via a pair rule circuit in *T. castaneum* [39]. After *zld* RNAi the characteristic *Tc-eve* stripe expression in the growth zone is lost. (Q,R) Segment generation from the growth-zone (GZ) is disrupted, as judged by the analysis of *Tc-gsb* expression after *Tc-zld* pRNAi (R) and *dsneo* (Q). (S,T) *Tc-zld* dsRNA embryonic injection (eRNAi) into nuclear GFP transgenic line affects segment generation from the posterior GZ (L-asterisk), when compared to nGFP embryo injected with *dsneo* dsRNA.

https://doi.org/10.1371/journal.pgen.1006868.g005

non-overlapping, dsRNA construct (S1 Fig). Further, morphological analyses showed that cellularization was severely disrupted in over 50% of the *zld* dsRNA embryos (Fig 5D), similarly to what was previously reported in *D. melanogaster zld* mutants [6, 11]. The remaining *zld* pRNAi embryos were not severely affected during cellularization and developed beyond that stage. Finally, we also found that some putative conserved target genes were down-regulated in embryos after *zld* pRNAi, such as the early zygotic genes involved in AP patterning, the serosal gene *Tc-zerknullt* [36] (Fig 5E and 5F) and the gap gene *milli-pattes* [37] (Fig 5G and 5H).

Changes in the spatial distribution of transcripts from predicted dorsoventral target genes were also observed after *Tc-zld* RNAi. In wild-type (WT) embryos, the TF Dorsal forms a dynamic transient gradient, which activates *Tc-cactus* (*Tc-cact*) and *Tc-short-gastrulation (Tc-sog*) at the ventral region [38, 39]. After *Tc-zld* pRNAi, the expression of *Tc-cact* and *Tc-sog* is observed in two lateral domains, in contrast to the expression at the single ventral domain in *dsneo* RNAi embryos (Fig 5I, 5J, 5K and 5L). These results suggest that *Tc-zld* is required for proper activity of Dorsal at the ventral-most region of the embryo.

As discussed above, *Tc-zld* is highly expressed at the posterior region of the embryo (Fig 3) and likely associated with segmentation and regionalization (S4 Table). Further, several putative *Tc-zld* targets are involved in posterior segmentation, such as *caudal (Cdx)*, *even-skipped (Eve)* and several Hox genes (e.g. *Ultrabithorax*, *Abdominal-A* and *Abdominal-B*). *Tc-eve*, for example, is essential for the establishment of a genetic circuit required for posterior segmentation [40]. Interestingly, *Tc-zld* pRNAi embryos showed a continuous *Tc-eve* expression domain instead of the typical stripe patterning required for WT segmentation (Fig 5O and 5P).

Elegant studies on *T. castaneum* GZ patterning showed that cell proliferation is not essential for segment generation, which rather occurs by coordinated cell movement and intercalation [19, 41]. We then evaluated whether *Tc-zld* regulates genes involved in cell intercalation, such as *Toll2*, *Toll6* and *Toll8* [42, 43]. Interestingly, *Toll7* (TC004474) and *Toll8* (*Tollo*:TC004898) are among the common *zld* targets conserved between *D. melanogaster* and *T. castaneum* (S3 Table). Since *Tc-Toll7* is expressed during early segmentation [43], we compared its expression in *dsneo* and *Tc-zld* RNAi embryos. While anterior expression of *Tc-Toll7* is apparently unaffected, the striped expression at the posterior region is lost when *Tc-zld* expression is reduced (Fig 5M and 5N). Further support for the loss of posterior segmentation after *Tc-zld* RNAi is also provided by the analysis of expression of the segment-polarity gene, *Tc-gooseberry* (*Tc-gsb*) (Fig 5Q and 5R). In summary, *Tc-zld* regulates the expression of several genes that are critical for early AP (*zen*, *mlpt*) and DV (*sog*, *cact*) patterning and, in a second phase, genes required for posterior elongation (e.g. *Toll7*, *gsb*).

Tc-zld plays specific roles in the posterior GZ

While pRNAi diminishes maternal and zygotic expression of *Tc-zld* in *T. castaneum* [15], embryonic dsRNA injections (eRNAi) may affect only the zygotic component, since eggs can

be injected after the MZT [38, 44]. To investigate if *Tc-zld* is specifically required for embryonic posterior patterning, we injected *Tc-zld* dsRNA in transgenic embryos expressing nuclear GFP (nGFP), as previously described [18, 19]. Embryonic injections of *Tc-zld* dsRNA after the MZT (see Methods for details) impaired segment generation from the GZ, while *dsneo*-injected embryos developed like WT ones (Fig 5S and 5T, S1 and S2 Movies). In addition, expression of the predicted target *Tc-eve*, a key TF involved in GZ patterning [35], has been largely down-regulated upon *Tc-zld* eRNAi, as previously observed for *zld* pRNAi (Fig 5O and 5P). In summary, our results imply that *Tc-zld* is involved not only in the MZT, early patterning and nervous system formation, as described for *D. melanogaster* [6], but also play roles in segment generation from the GZ, a structure found only in embryos of short-germ insects like *T. castaneum*.

Functional analysis in the hemipteran *Rhodnius prolixus* shows a conserved role of *zld* in short-germ insect posterior region

Although we demonstrated the involvement of *zld* in *T. castaneum* GZ, the conservation of this regulatory mechanism in other species remained unclear. Thus, we sought to analyze the functions of the *zld* ortholog in the hemipteran *R. prolixus* (*Rp; Rp-zld* gene), which is a hemimetabolous insect and lacks the complete metamorphosis present in holometabolous species such as *T. castaneum* [45, 46]. *Rp-zld* knockdown via pRNAi resulted in two types of embryonic phenotypes: 1) severe defects in gastrulation and lack of any appendage development; 2) embryos that developed only the anterior-most embryonic regions comprising the head, gnathal and thoracic segments (Fig 6). These results support a role for *zld* in posterior elongation that was likely present in the common ancestor of hemimetabolous true bugs and holometabolous insects, if not earlier. To our knowledge this is the first direct description of *zld* function in insects other than *D. melanogaster*. A recent report showed *zld* as maternally transcribed in the hymenoptera *Apis mellifera* (also a long-germ insect), while zygotic transcripts are concentrated at the central region of the embryo during blastodermal stages [47]. Further, during the preparation of this manuscript, *zld* has been also proposed to be required for MZT and cellularization in the wasp *Nasonia vitripennis* [48].

Tc-zld is essential for patterning of imaginal disc-derived structures: Wing, legs, elytra and antenna

DAVID analysis of *D. melanogaster* orthologs of the putative *Tc-zld* targets uncovered a cluster of 29 genes involved in imaginal disc development (S4 Table; GO:0007444). Among these genes are several homeodomain TFs, such as *distalless* (*Dll*), *Abdominal A* (*Abd-A*), *Abdominal B* (*Abd-B*), *zen*, *Engrailed* (*En*), *caudal* (*cad*), *defective proventriculus* (*dve*), *mirror* (*mirr*), *araucan* (*ara-iroquois*) and *Drop* (*dr*), as well as other TFs such as *dachsund* (*dac*), *taranis* (*tara*) and *Lim1*, *PoxN*, *kn*, *sob*, *drm*, *Awh*, *dp*.

As the first step towards the characterization of the post-embryonic role of *zld*, we analyzed *Tc-zld* expression by qRT-PCR in larvae of third (L3), fifth (L5) and seventh (L7) stages, and first pupal stage (P1) (Fig 7A–7D). Interestingly, *Tc-zld* expression increases during successive larval stages and sharply decreases after pupal metamorphosis (Fig 7E). This suggests that *Tc-zld* might be required for late larval stages, which take place during larvae-pupae metamorphosis, such as growth and patterning of structures derived from imaginal discs in *D. melanogaster* (e.g. antennae, legs, fore- and hindwings) [49, 50]. Further, we found that three out of five predicted *Tc-zld* targets, namely *Dll*, *Wg* and *Lim-1*, also displayed an increase in expression during late larval and pupal development (Fig 7E).

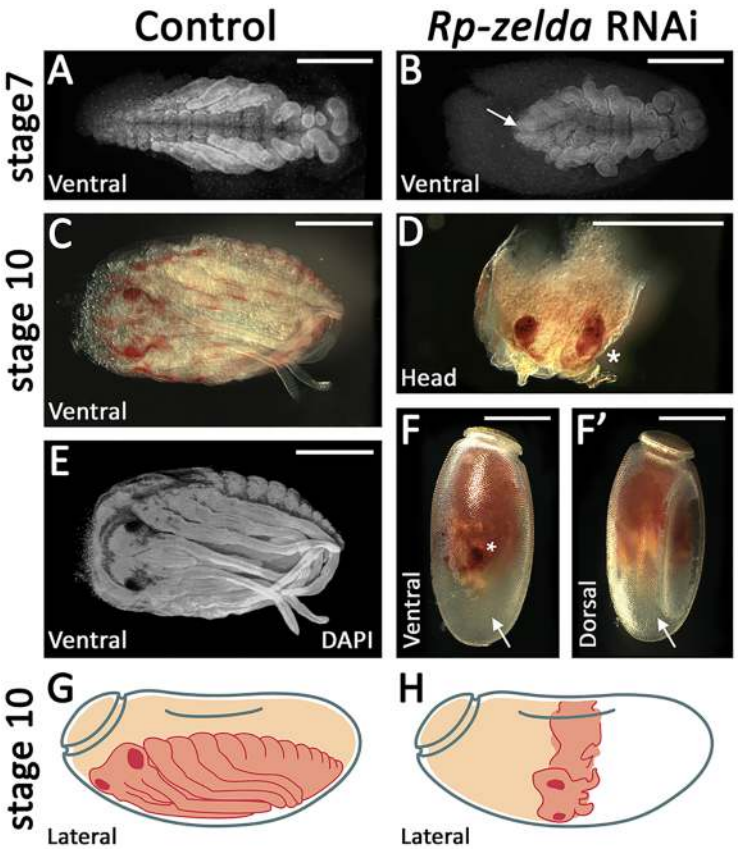

Fig 6. *zld* is required for the generation of the posterior region in the hemiptera *Rhodnius prolixus*. (A, C,E) *R. prolixus* control (*dsneo* embryos). (B,D,F,F') A representative embryo collected from *R. prolixus zld* pRNAi. (F,F') Embryo inside the chorion, ventral and dorsal views. (C,E) Embryo removed from the egg shell. (G,H) Schematic drawings of control and *zld* pRNAi embryos. (A) DAPI stainings of control (A,E) and *zld* RNAi (B) embryos. (D) Asterisk denotes an eye which can be observed at the ventral side (F). (D) After dissection, the eye can be identified due to its characteristic red pigmentation and shape. Scale bar corresponds to 500μM.

https://doi.org/10.1371/journal.pgen.1006868.g006

To investigate *zld´s* post-embryonic roles, we injected two non-overlapping *Tc-zld* dsRNA constructs into early (L3) and late larval (L6) stages, as previously described [50]. qRT-PCR confirmed that *Tc-zld* was down-regulated after dsRNA injection (Fig 8A). *Tc-zld* dsRNA injections at early larval stages (L3) led to over 50% lethality during pupal stages. Atypical adult pigmentation in the pupal head and reduction in the wing size were observed after early *Tc-zld* dsRNA injection, suggesting that proper *Tc-zld* expression is required for metamorphosis and wing growth (Fig 8B and 8C). Interestingly, *Tc-zld* dsRNA injections at late larval stage (L6) displayed a different phenotype when compared with early larval dsRNA injections (L3). L6 larvae injected with *dszld* and *dsneo* reached adulthood at comparable rates (Fig 8D). Specifically, *Tc-zld* dsRNA adults showed a series of morphological alterations in tissues undergoing extensive morphological changes during metamorphosis, such as fore- and hindwings, antennae and legs (Figs 8E, 8F, 9 and 10).

The most visible effect of *Tc-zld* dsRNA beetles was a failure of the forewings (elytra) to enclose the hindwings, leading to the exposure of the dorsal abdomen (Fig 8E and 8F). Elytra, which are highly modified beetle forewings, have been proposed to be an important beetle innovation, being required for protection against mechanical stresses, dehydration, and

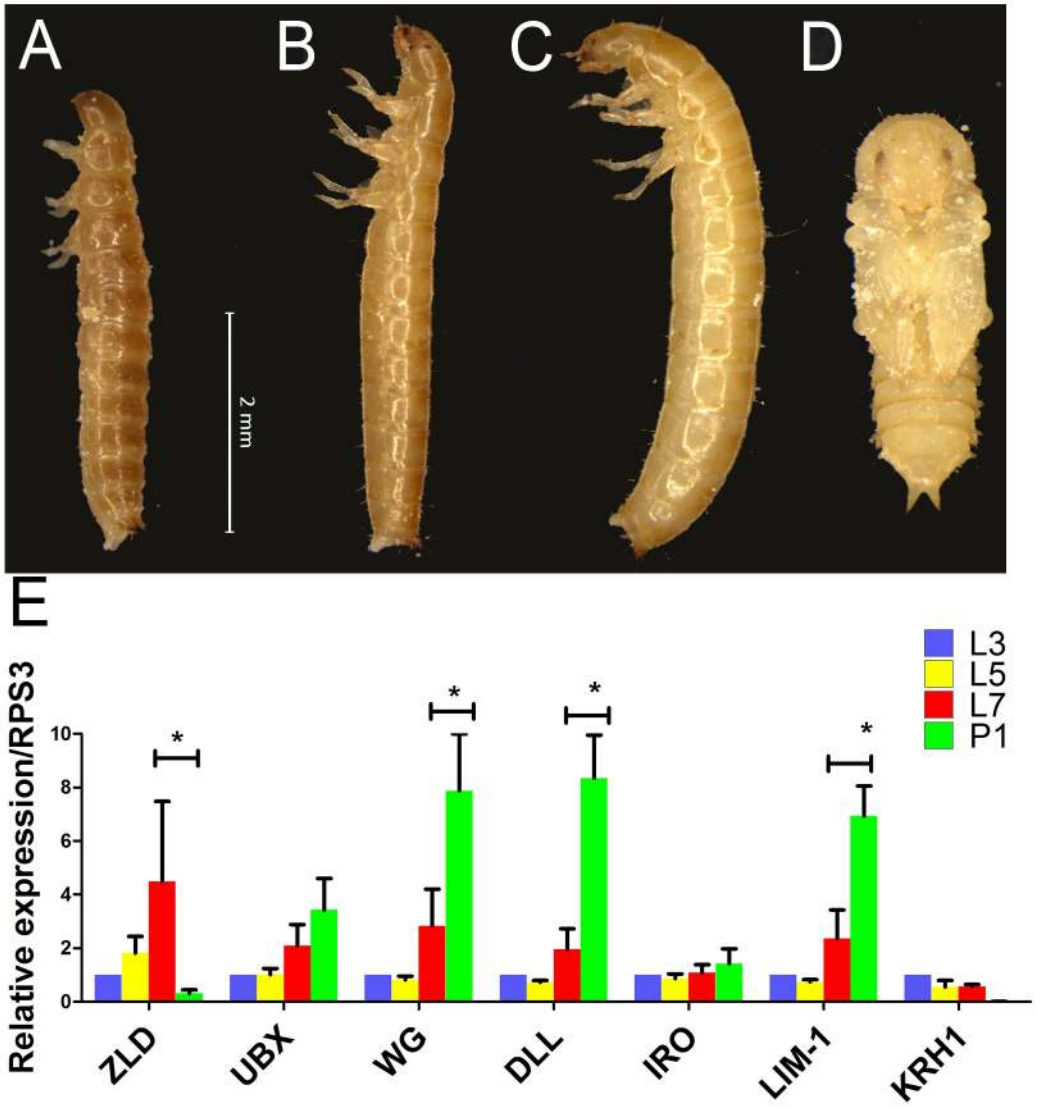

Fig 7. Larval stages and expression dynamics of *zld* and its putative target genes. (A-D) Morphology of *Tribolium castaneum* larvae on 3rd (A-L3), 5th (B-L5), 7th (C-L7) and early pupal stages (D-P1). (E) Relative expression of *zld*, *Ubx*, *wingless (wg)*, *distalless (dll)*, *Iroquois (iro)*, *Lim-1* and *Kruppel-homolog-1 (KRH-1)* at L3, L5, L7 and P1. Asterisks represent significant differences between stages (P<0.05).

https://doi.org/10.1371/journal.pgen.1006868.g007

predation [51]. In line with this hypothesis, *Tc-zld* dsRNA adults with exposed abdomens started to die a few days after metamorphosis, probably due to dehydration.

Next, we performed a detailed morphological analysis to investigate if patterning defects resulting from *Tc-zld* dsRNA occurred in the sclerotized elytra (forewing) or in the hindwing (Fig 9A–9D). This analysis showed that the parallel vein pattern of the elytra (Fig 9A) is disrupted after *Tc-zld* dsRNA in comparison to the control (Fig 9A and 9B). Nevertheless, hindwings of *Tc-zld* dsRNA beetles showed no signs of abnormal venation (Fig 9C and 9D). To address if fore or hindwing shapes have changed upon *Tc-zld* dsRNA knockdown, we applied the recently developed Proximo-Distal (PD) index, a morphometric analysis consisting of the measurement of the wing length and width at two positions [52]. While the PD index values of forewings (elytra) of *Tc-zld* and controls were similar, a slight but significant increase in the

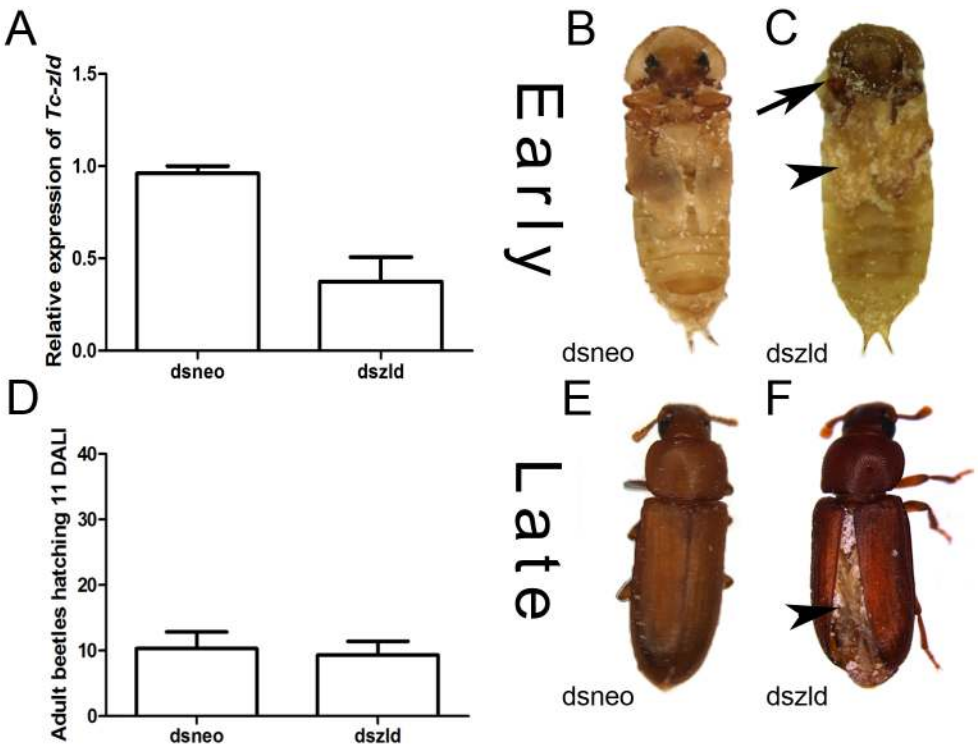

Fig 8. *Tc-zelda* larval RNAi affects elytra enclosure and molting. *Tribolium castaneum* larvae were injected during early (3rd) and late (6th) stages as previously described [50, 80]. (A) Relative expression of *Tc-zld* during pupal stages after *Tc-zld* dsRNA or *neo* dsRNA injection. qRT-PCR was normalized using *Tc-rps3* gene, as previously described [78]. (B,C) Morphology of late pupae obtained from early larvae injected with *zld* or *neo* dsRNA. Differential pigmentation in the head (arrow) and reduced wings (arrowhead) were observed in *zld* dsRNA and not in *dsneo* dsRNA pupae. (D) Number of emerging adult beetles eleven days after larval injection (DALI) at late (6th) stage. (E,F). Adults obtained by late larval injections of *neo* (E) or *zld* (F) dsRNA. Hindwings are usually not properly folded underneath the forewing (elytra).

https://doi.org/10.1371/journal.pgen.1006868.g008

hindwing PD index was observed (Fig 9E). Neither fore- nor hindwings length were altered upon *Tc-zld* knock down (Fig 9F). In conclusion, *Tc-zld* is required for proper venation pattern, but not shape, of the elytra. Previous analysis of *zld* expression in *D. melanogaster* showed expression in wing imaginal discs, particularly where mitotically active cells are located [11]. Moreover, *Dm-zld* overexpression during wing imaginal disc formation leads to adult wing blisters or tissue loss [10, 11]. Nevertheless, to our knowledge, our study provides the first direct evidence of *zld*′s role in insect wing formation.

Interestingly, all *Tc-zld* dsRNA beetles that showed this 'opened wing' phenotypes (Fig 8F) also displayed defects in the legs and antennae. Antennae and legs share similar developmental GRNs, involving the so called serial homologs. *Distaless (Dll)*, one of the putative *Tc-zld* targets, is essential for appendage segmentation [53]. *Tc-Dll* is also expressed during late embryogenesis on the distal part of the leg and, as its name suggests, disruption of its function leads to the absence of distal leg and antennae segmentation [54]. Interestingly, we found that *Tc-zld* RNAi resulted in a significant decrease of *Tc-Dll* mRNA levels (Fig 10A), indicating that this gene is indeed downstream of *Tc-zld*.

Insect antennae possess three primary segments: scape, pedicel and flagellum. In *T. castaneum*, the adult antennae display eleven segments, out of which nine form the flagellum. The three most distal flagellar segments are enlarged and form the club, while the six intermediate

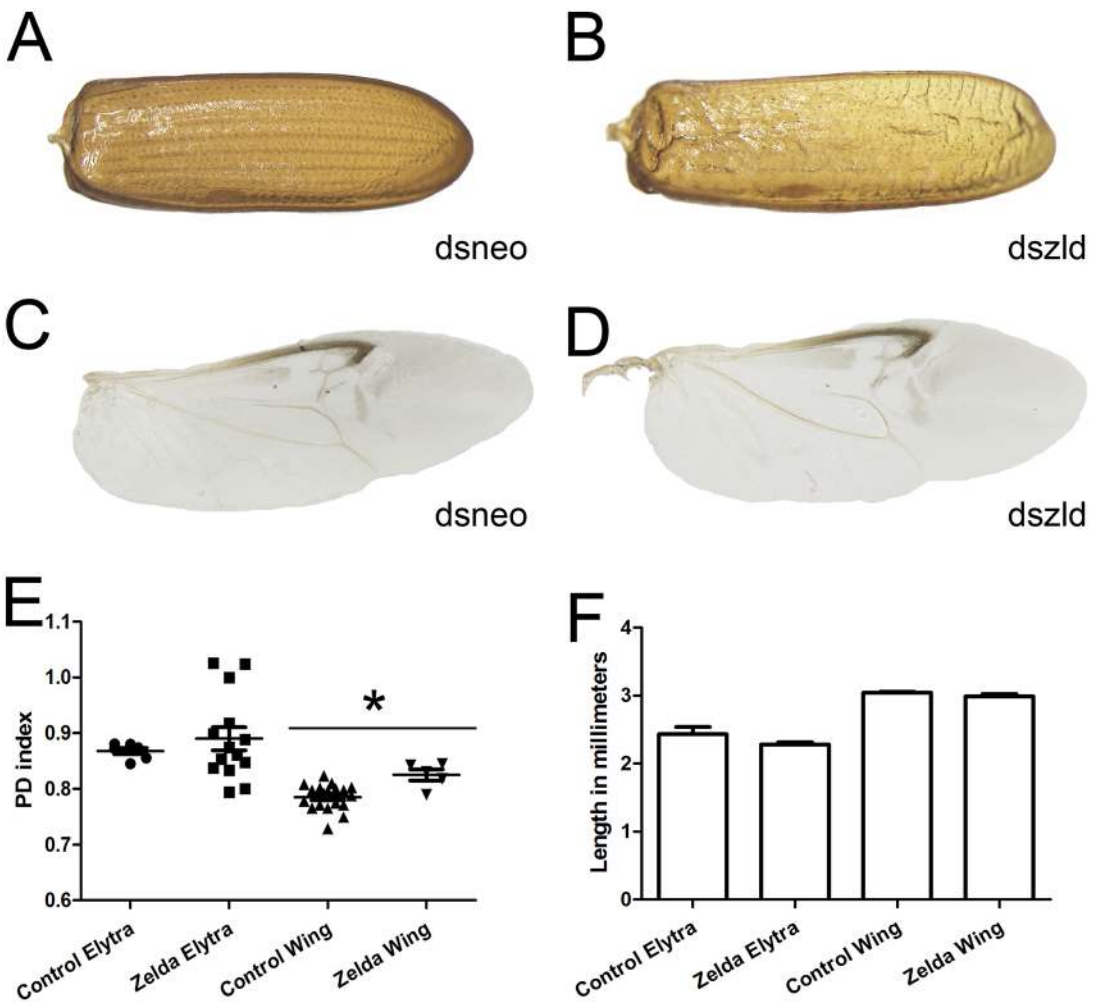

Fig 9. *Tc-zld* knockdown in larval stages affects elytra and wings in adult stage. (A) Control elytron extracted from a *dsneo* adult shows a parallel venation pattern and rigid chitinous structure. (B) *Tc-zld* RNAi elytron displays a disrupted vein pattern and a less resistant structure. (C,D) Hindwings were dissected and photographed. Although the overall morphological pattern is not affected in both wings, *zld* dsRNA wings show severe dehydration after ethanol fixation. (E) PD indexes comparison between *dsneo* and *dszld* RNAi hindwings and forewings, a PD index reflects the shape of the wing based on its dimensions ratio [52]. The statistical analysis was carried out by unpaired t-test assuming unequal variances (asterisks refer to P<0.0001 while ns stands for "no significance"), indicating that *Tc-zelda* RNAi affects hindwing shape. (F) *Tc-zld* RNAi elytra and hindwing do not show statistically significant differences in length when compared to their respective *dsneo* RNAi controls.

https://doi.org/10.1371/journal.pgen.1006868.g009

flagella are called the funicle (Fig 10B) [55]. In mild phenotypes, *dszld* caused a joint malformation in distalmost flagellar segments resulting in a fusion of the club (Fig 10C). On the other hand, strong *Tc-zld* dsRNA phenotypes resulted in fusion of the scape and pedicel, leading to severe loss of flagellar joints and formation of a single truncated segment (Fig 10D). In contrast, no differences in scape and pedicel were observed.

T. castaneum legs originate during late embryogenesis and can be recognized as a small outgrowth of the body wall, the limb bud. In the adult stage, there are three pairs of segmented legs with six segments: coxa, femur, trochanter, tibia, tarsus and pretarsus [56]. In *T. castaneum* the tarsus is subdivided in smaller segments (i.e. the tarsomeres), five in prothoracic and mesothoracic legs and four in metathoracic legs. Tarsal segmentation occurs during beetle

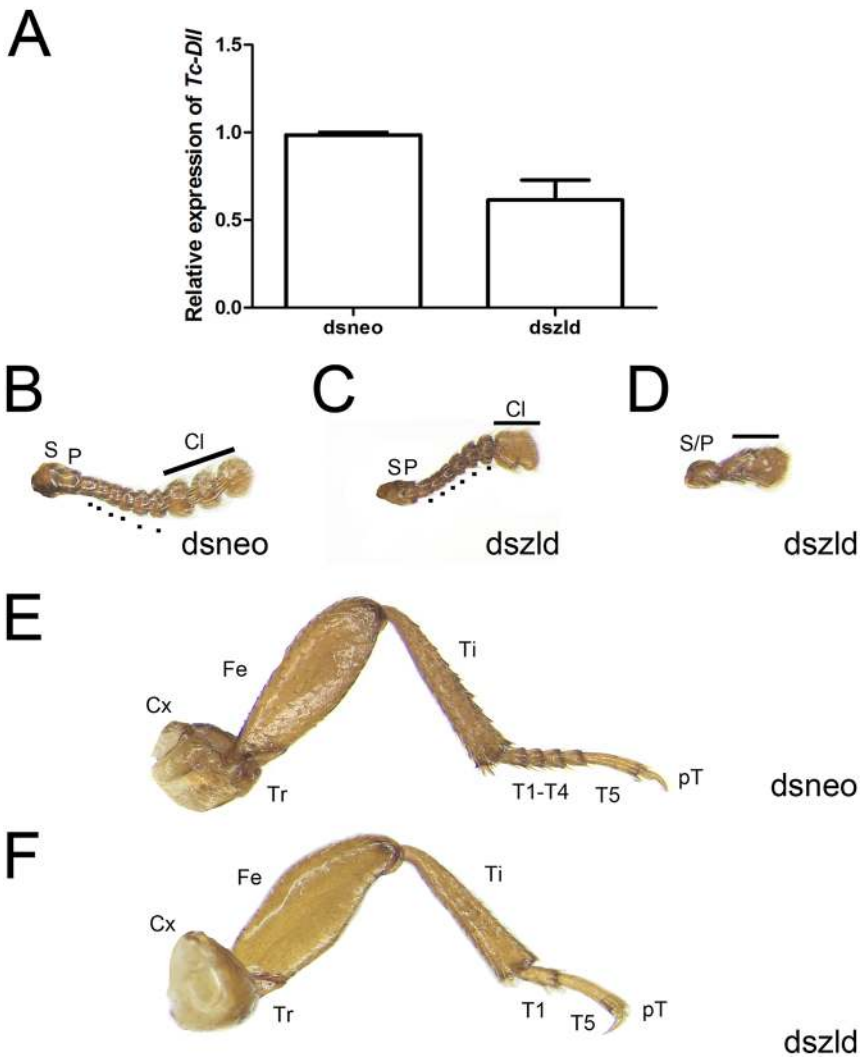

Fig 10. *Tc-zld* knockdown induces phenotypes in antennae and legs of adult *T. castaneum*. (A) Relative expression of *Tc-Dll* at pupal stages after *neo* or *zld* dsRNA injections. (B-D) Antennae extracted from control injected individuals (B) display 11 segments, including two proximal (S = scape, P = pedicel), six intermediate (Flagellum = dots) and three distal modified segments that form the club (Cl). (C,D) Injection of *zld* dsRNA caused fusion of the club segments in mild phenotypes (C), while in stronger phenotypes (D) the antennae fail to segment, developing as an antennal rudiment. (E,F) Legs of *T. castaneum* display six podomeres: Coxa (Cx), Trochanter (Tr), Femur (Fe), Tibia (Ti), Tarsus (T) and pretarsus (pT). (E) Mesothoracic legs of *neo* dsRNA injected individuals show five tarsal segments, or tarsomeres. (F) *zld* dsRNA beetles lacks tarsal segments resulting in a reduced tarsus, while other leg structures do not display large morphological defects.

https://doi.org/10.1371/journal.pgen.1006868.g010

metamorphosis and this subdivision of the tarsus evolved in the common ancestor of insects, since the tarsus is not subdivided in non-insect hexapods [57]. After *Tc-zld* RNAi, tarsal segments were absent or fused, resulting in leg shortening; in *dsneo* insects, legs were identical to that of WT animals (Fig 10E and 10F). This indicates that some of the *Tc-zld* targets are involved in segment development or joint formation. Interestingly, a large domain of *Dll* expression is observed in beetle leg tarsus [58], and *Tc-Dll* knockdown in beetles also generated legs with tarsomere deletion [58, 59].

zld is required for diverse biological processes during embryonic and postembryonic development

Besides the conservation of *zld* roles in the MZT, our results uncovered two new biological roles of *zld* in *T. castaneum*: regulation of segment generation from the posterior GZ during embryogenesis and; patterning of imaginal disc derived structures. But what do posterior GZ patterning, MZT and imaginal disc development have in common? All these processes require an accurate temporal and spatial coordination of complex GRNs to properly pattern cell populations.

Recently, *Dm-zld* has been demonstrated to be a key factor in the establishment of the early chromatin architecture, particularly for the formation of topologically associating domain (TAD) boundaries [60]. During *D. melanogaster* MZT, *zld* resembles a pioneer TF marking the chromatin of earliest expressed genes [8, 61]. *Dm-zld* also increases chromatin accessibility of the most important TFs involved in DV and AP patterning (*Dorsal* and *Bicoid*, respectively) [62–65]. Further, the addition or removal of *Dm-zld* binding sites influences the timing of activation of Dorsal early zygotic targets in *D. melanogaster* [62, 63], suggesting that Zld acts as a developmental timer.

Our results in *T. castaneum* showed an extensive and ubiquitous maternal contribution of *Tc-zld* mRNAs, followed by zygotic *Tc-zld* expression along the embryonic rudiment, particularly at the posterior region (Fig 3). It is possible that *Tc-zld* mediates a progressive anteroposterior opening of the chromatin in *T. castaneum*, shortly before these posterior GZ cells undergo convergent extension movements required for germ band elongation [19, 41]. Loss of *Tc-zld* expression might lead to lack of convergent extension due to loss of *Toll7* and *eve* expression and, ultimately, segmentation failure (Fig 5). Since *zld* is also important for the development of the posterior region of the hemimetabolous insect *R. prolixus* (Fig 6), *zld´s* role in posterior region dates back at least to the last common ancestor of Paraneoptera.

Tc-zld expression was also observed at the ventral serosa (Fig 3J) during embryonic stages. While we cannot rule out that *Tc-zld* plays a role during normal serosal development, lack of segmentation after *Tc-zld* eRNAi cannot be explained by loss of *Tc-zld* expression in this tissue, since embryos without serosa, e.g. *Tc-zen1* RNAi, do not display phenotypic defects under normal developmental conditions [36, 66]. Future studies are warranted to determine if *Tc-zld* plays a specific role in the beetle serosa, particularly by regulating some of its predicted target genes involved in immune responses (e.g. *Toll*, *cactus*).

Tc-zld might also play a similar role in the regulation of leg and antenna segmentation during metamorphosis (Fig 10). The number of tarsomere segments in the leg and intermediate funicle are reduced after *Tc-zld* dsRNA injection, suggesting that the post-embryonic role of *Tc-zld* in appendage segmentation might also involve the regulation of complex GRNs, as observed in the posterior embryonic region.

The evolutionary success of hexapods is attributed to a combination of features: their segmented body plan and jointed appendages, which were inherited from their arthropod ancestor and; wings and holometaboly, two features that arose later in insect evolution [67]. It is interesting to note that the specific Pancrustacea gene *zld* is required for most of these processes, such as embryonic segment formation, wing (elytra) patterning, and appendage (antennae and leg) formation during beetle development. Like several other zinc finger proteins that show tremendous lineage-specific diversity in eukaryotes, *zld* appears to have specifically arisen within Pancrustacea and risen to play an important role as a "master TF". Hence, future studies focusing on how this TF was integrated to the conserved backdrop of developmental TFs and existing GRNs of arthropods would be of great interest.

Materials & methods

Beetle rearing

T. castaneum beetles were cultivated in whole-wheat flour. For sterilization, the flour was kept for 24h at -20˚C and another 24h at 50˚C. The beetles were maintained inside plastic boxes of approximately 15x15cm with humidity between 40–80%.

Bioinformatic analyses

Protein sequence analyses were performed using BLAST [68] and PFAM searches using HMMER3 [69] against proteins available on Genbank [70] and Vectorbase [71]. Dm-Zld (NP_608356) was used as initial query for sequence searches. Genomic data from the following genomes were obtained from the Baylor College of Medicine Human Genome Sequencing Center: *Eurytemora affinis*, *Hyalella azteca*, *Blattella germanica*, *Catajapyx aquilonaris*, *Machilis hrabei*, *Libellula (Ladona) fulva* and *Ephemera danica*. BLAST results and domain architectures were manually inspected. *In silico* searches in the *T. castaneum* genome for over-represented motifs were performed using the DREME software [72], part of the MEME suite software toolkit [73]. The motif with highest identity with Dm-Zld binding site (CAGGTAY) was compared to previously described motifs in the FlyFactorSurvey [74] database with TOMTOM. Further, this motif was used to scan 2000 bp upstream of all predicted *T. castaneum* genes with FIMO [14, 75, 76]. Upstream regions and orthology information were retrieved from Ensembl Metazoa Biomart (http://metazoa.ensembl.org/biomart/) [77].

dsRNA synthesis, parental RNAi and embryonic phenotypic analysis

Two non-overlapping PCR fragments containing T7 promoter initiation sites at both ends were used as templates for Ambion T7 Megascript Kit (Cat. No. AM1334) following the manufacturer instructions (for details see S1 Fig). The amount and integrity of the dsRNA samples were measured by spectrophotometry and agarose gel electrophoresis, respectively. For parental RNAi (pRNAi) analysis, ~0.5μl of dsRNA were injected from a solution containing 1μg/μl of dsRNA into adult female beetles [36]. Eggs were collected for four egg lays (2 day each) and *zld´s* down regulation was estimated by quantitative Real Time PCR (see below).

T. castaneum embryonic dsRNA injections

Egg injections were performed as previously described [38, 44]. Briefly, for the analysis of *Tc-zld* zygotic role, embryos containing nuclear-localized green fluorescent protein (GFP) were collected for one hour and let to develop for an additional three hours (30˚C) [19, 35]. After this period, twenty embryos were dechorionated with bleach (2% solution), aligned onto a glass slide and covered with Halocarbon oil 700 (Sigma). Embryos were immediately microinjected at the anterior region with *zld* or *neo* dsRNA at 1 μg/μL concentration with the help of a Nanoinject II instrument (Drummond Scientific Company). After injection, a single nGFP embryo was photographed every five minutes during the following 16 hours (25˚C) in a Leica DMI4000 inverted microscope using a GFP filter. Single photographs were used to generate a movie using Windows Movie Maker (S1 and S2 Movies). Phenotypes of all injected embryos (*neo* or *zld* dsRNA) were scored at the end of the experiment.

T. castaneum larval dsRNA injections

Larvae were injected with *zld* or *neo* dsRNA as previously described [50]. Knockdown phenotypes in pupae and adult beetles were generated by injection of *zld* or *neo* dsRNA solutions at a concentration of 1 μg/μL in the dorsal abdomen of individuals on third and sixth larval instars

(n = 40). Following injection, larvae were reared in flour at 30˚C and collected periodically for RNA extraction and phenotype annotation. Adult beetles were then fixed in ethanol 95% overnight for further morphological analysis. Immunostainings have been performed as previously described [38].

Morphological analysis of imaginal disc derived tissues

Antennae, legs, elytra and wings were dissected using forceps and placed in a petri dish for observation. Phenotypic analyses and documentation were performed under a Leica stereoscope model M205.

PD index

The methods for wing and elytra measurement and PD index were performed according to described by [52]. Leica AF Lite software was used for the wing measurements. Image properties were adjusted in Adobe Photoshop CS4.

Quantitative real-time PCR

For experiments using embryos, total RNA was isolated from 100 mg of eggs collected from specific development stages (0–3, 3–6 and 6–9 hours after egg laying), ovary and carcass (whole beetle without ovary) using Trizol (Invitrogen), according to the manufacturer's instructions. Three independent biological replicates were used for each assay. First strand complementary DNA (cDNA) was synthesized from 2 μg of RNA using Superscript III reverse transcriptase (Invitrogen) and oligo(dT). The cDNA was used as template for real time qRT-PCR analysis using SYBR green based detection. qRT-PCR reactions were carried out in triplicate, and melting curves were examined to ensure single products. Results were quantified using the "delta-delta Ct" method and normalized to *rps3* transcript levels, as previously described [78]. Primer sequences used during the study are provided at the supplemental data (S5 Table).

zld pRNAi in the hemiptera *Rhodnius prolixus (Rp)*

zld cDNA sequence was initially identified by BLAST and included in Fig 1. Parental RNAi against *Rp-zld* was performed as previously described [46].

Supporting information

S1 Fig. Schematic drawings of *Tc-zelda* non-overlapping dsRNA constructs. *Tc-zld* gene corresponds to the Beetlebase ID: TC014798. The following primer pairs were used: C1-Forward ggccgcggAGCGCATCTTCTCCCTATCA and C1-Reverse cccggggcGCCGTTTTGT CGTTTCTCAT. This primer pair amplifies leads to the amplification of a fragment of 528 bp (349–857). A second primer pair C2-Forward ggccgcggACGACGAGTACCGCTTGACT and C2-Reverse—cccggggcCTTACCACAGGTGTCGCAGA was also used and lead to similar results. This primer pair amplifies a fragment of 476 bp (1823–2279) covering the four zinc-finger domains. The lowercase letters contain the primer sequence used as a template for a second PCR using universal primers which adds a T7 promoter at both sides of the PCR template as previously described [81].
(TIF)

S1 Table. Zelda homologs in several Pancrustacea species.
(XLSX)

S2 Table. Gene IDs of 3250 genes with the motif GTAGGTAY in the 2kb upstream regions of *T. castaneum genes* protein-coding genes.
(XLS)

S3 Table. List of 141 *Dm-zld* targets during the MZT with one-to-one orthologs among *Tc-zld* predicted targets.
(XLS)

S4 Table. DAVID functional analysis and enriched ontology terms of the genes listed in S3 Table.
(XLS)

S5 Table. Primers used in quantitative qRT-PCR experiments.
(XLSX)

S1 Movie. A representative nGFP embryo injected with *dsneo* dsRNA (see Methods for a detailed description).
(MP4)

S2 Movie. A representative nGFP embryo injected with Tc-zld dsRNA (see Methods for a detailed description).
(MP4)

Acknowledgments

RNdaF would like to thank Prof. Michalis Averof for providing the nuclear GFP line and Prof. Siegfried Roth (Univ. Cologne, Germany) for the support during the beginning of this project.

Author Contributions

Conceptualization: Thiago M. Venancio, Rodrigo Nunes da Fonseca.

Data curation: Thiago M. Venancio, Rodrigo Nunes da Fonseca.

Formal analysis: Lupis Ribeiro, Vitória Tobias-Santos, Thiago M. Venancio, Rodrigo Nunes da Fonseca.

Funding acquisition: L. Aravind, Thiago M. Venancio, Rodrigo Nunes da Fonseca.

Investigation: Lupis Ribeiro, Vitória Tobias-Santos, Daniele Santos, Felipe Antunes, Geórgia Feltran, Jackson de Souza Menezes, L. Aravind, Thiago M. Venancio, Rodrigo Nunes da Fonseca.

Methodology: Lupis Ribeiro, Daniele Santos, Felipe Antunes, Geórgia Feltran, Jackson de Souza Menezes, L. Aravind, Thiago M. Venancio, Rodrigo Nunes da Fonseca.

Project administration: Thiago M. Venancio, Rodrigo Nunes da Fonseca.

Resources: Thiago M. Venancio, Rodrigo Nunes da Fonseca.

Software: Lupis Ribeiro, L. Aravind, Thiago M. Venancio.

Supervision: Jackson de Souza Menezes, Thiago M. Venancio, Rodrigo Nunes da Fonseca.

Validation: Lupis Ribeiro, Vitória Tobias-Santos, Daniele Santos, Felipe Antunes, Geórgia Feltran, Jackson de Souza Menezes, L. Aravind, Thiago M. Venancio, Rodrigo Nunes da Fonseca.

Visualization: Lupis Ribeiro, Vitória Tobias-Santos, Daniele Santos, Geórgia Feltran, Jackson de Souza Menezes, L. Aravind, Thiago M. Venancio, Rodrigo Nunes da Fonseca.

Writing – original draft: Lupis Ribeiro, Thiago M. Venancio, Rodrigo Nunes da Fonseca.

Writing – review & editing: Lupis Ribeiro, L. Aravind, Thiago M. Venancio, Rodrigo Nunes da Fonseca.

References

1. Nowick K, Stubbs L. Lineage-specific transcription factors and the evolution of gene regulatory networks. Briefings in functional genomics. 2010; 9(1):65–78. https://doi.org/10.1093/bfgp/elp056 PMID: 20081217
2. Aravind L, Anantharaman V, Venancio TM. Apprehending multicellularity: regulatory networks, genomics, and evolution. Birth Defects Research Part C, Embryo Today: Reviews. 2009; 87(2):143–64. https://doi.org/10.1002/bdrc.20153 PMID: 19530132
3. Kvon EZ, Kazmar T, Stampfel G, Yáñez-Cuna JO, Pagani M, Schernhuber K, et al. Genome-scale functional characterization of Drosophila developmental enhancers in vivo. Nature. 2014; 512(7512):91–5. https://doi.org/10.1038/nature13395 PMID: 24896182
4. Blythe SA, Wieschaus EF. Coordinating Cell Cycle Remodeling with Transcriptional Activation at the Drosophila MBT. Current Topics in Developmental Biology. 2015; 113:113–48. https://doi.org/10.1016/bs.ctdb.2015.06.002 PMID: 26358872
5. Tadros W, Lipshitz HD. The maternal-to-zygotic transition: a play in two acts. Development. 2009; 136 (18):3033–42. https://doi.org/10.1242/dev.033183 PMID: 19700615
6. Liang H-L, Nien C-Y, Liu H-Y, Metzstein MM, Kirov N, Rushlow C. The zinc-finger protein Zelda is a key activator of the early zygotic genome in Drosophila. Nature. 2008; 456(7220):400–3. https://doi.org/10.1038/nature07388 PMID: 18931655
7. De Renzis S, Elemento O, Tavazoie S, Wieschaus EF. Unmasking activation of the zygotic genome using chromosomal deletions in the Drosophila embryo. PLoS Biology. 2007; 5(5):e117. https://doi.org/10.1371/journal.pbio.0050117 PMID: 17456005
8. Harrison MM, Li X-Y, Kaplan T, Botchan MR, Eisen MB. Zelda binding in the early Drosophila melanogaster embryo marks regions subsequently activated at the maternal-to-zygotic transition. PLoS Genetics. 2011; 7(10):e1002266. https://doi.org/10.1371/journal.pgen.1002266 PMID: 22028662
9. ten Bosch JR, Benavides JA, Cline TW. The TAGteam DNA motif controls the timing of Drosophila preblastoderm transcription. Development. 2006; 133(10):1967–77. https://doi.org/10.1242/dev.02373 PMID: 16624855
10. Giannios P, Tsitilou SG. The embryonic transcription factor Zelda of Drosophila melanogaster is also expressed in larvae and may regulate developmentally important genes. Biochemical and Biophysical Research Communications. 2013; 438(2):329–33. https://doi.org/10.1016/j.bbrc.2013.07.071 PMID: 23891688
11. Staudt N, Fellert S, Chung H-R, Jäckle H, Vorbrüggen G. Mutations of the Drosophila zinc finger-encoding gene vielfältig impair mitotic cell divisions and cause improper chromosome segregation. Molecular Biology of the Cell. 2006; 17(5):2356–65. https://doi.org/10.1091/mbc.E05-11-1056 PMID: 16525017
12. Lynch JA, El-Sherif E, Brown SJ. Comparisons of the embryonic development of Drosophila, Nasonia, and Tribolium. Wiley interdisciplinary reviews Developmental biology. 2012; 1(1):16–39. https://doi.org/10.1002/wdev.3 PMID: 23801665
13. Davis GK, Patel NH. Short, long, and beyond: molecular and embryological approaches to insect segmentation. Annual Review of Entomology. 2002; 47:669–99. https://doi.org/10.1146/annurev.ento.47.091201.145251 PMID: 11729088
14. Tribolium Genome Sequencing C, Richards S, Gibbs RA, Weinstock GM, Brown SJ, Denell R, et al. The genome of the model beetle and pest Tribolium castaneum. Nature. 2008; 452(7190):949–55. https://doi.org/10.1038/nature06784 PMID: 18362917
15. Bucher G, Scholten J, Klingler M. Parental rnai in tribolium (coleoptera). Current Biology. 2002; 12(3): R85–6. PMID: 11839285
16. Schinko JB, Hillebrand K, Bucher G. Heat shock-mediated misexpression of genes in the beetle Tribolium castaneum. Development Genes and Evolution. 2012; 222(5):287–98. https://doi.org/10.1007/s00427-012-0412-x PMID: 22890852

17. Schinko JB, Weber M, Viktorinova I, Kiupakis A, Averof M, Klingler M, et al. Functionality of the GAL4/UAS system in Tribolium requires the use of endogenous core promoters. BMC Developmental Biology. 2010; 10:53. https://doi.org/10.1186/1471-213X-10-53 PMID: 20482875

18. Benton MA, Akam M, Pavlopoulos A. Cell and tissue dynamics during Tribolium embryogenesis revealed by versatile fluorescence labeling approaches. Development. 2013; 140(15):3210–20. https://doi.org/10.1242/dev.096271 PMID: 23861059

19. Sarrazin AF, Peel AD, Averof M. A segmentation clock with two-segment periodicity in insects. Science. 2012; 336(6079):338–41. https://doi.org/10.1126/science.1218256 PMID: 22403177

20. Panfilio KA, Oberhofer G, Roth S. High plasticity in epithelial morphogenesis during insect dorsal closure. Biology open. 2013; 2(11):1108–18. https://doi.org/10.1242/bio.20136072 PMID: 24244847

21. Kittelmann S, Ulrich J, Posnien N, Bucher G. Changes in anterior head patterning underlie the evolution of long germ embryogenesis. Developmental Biology. 2013; 374(1):174–84. https://doi.org/10.1016/j.ydbio.2012.11.026 PMID: 23201022

22. Handel K, Grunfelder CG, Roth S, Sander K. Tribolium embryogenesis: a SEM study of cell shapes and movements from blastoderm to serosal closure. Dev Genes Evol. 2000; 210(4):167–79. https://doi.org/10.1007/s004270050301 PMID: 11180819.

23. Vidal NM, Grazziotin AL, Iyer LM, Aravind L, Venancio TM. Transcription factors, chromatin proteins and the diversification of Hemiptera. Insect Biochemistry and Molecular Biology. 2016; 69:1–13. https://doi.org/10.1016/j.ibmb.2015.07.001 PMID: 26226651

24. Hamm DC, Bondra ER, Harrison MM. Transcriptional activation is a conserved feature of the early embryonic factor Zelda that requires a cluster of four zinc fingers for DNA binding and a low-complexity activation domain. The Journal of Biological Chemistry. 2015; 290(6):3508–18. https://doi.org/10.1074/jbc.M114.602292 PMID: 25538246

25. Drozdetskiy A, Cole C, Procter J, Barton GJ. JPred4: a protein secondary structure prediction server. Nucleic Acids Res. 2015; 43(W1):W389–94. https://doi.org/10.1093/nar/gkv332 PMID: 25883141;

26. Aravind L, Iyer LM. The HARE-HTH and associated domains: novel modules in the coordination of epigenetic DNA and protein modifications. Cell Cycle. 2012; 11(1):119–31. https://doi.org/10.4161/cc.11.1.18475 PMID: 22186017

27. Balaji S, Iyer LM, Aravind L. HPC2 and ubinuclein define a novel family of histone chaperones conserved throughout eukaryotes. Molecular Biosystems. 2009; 5(3):269–75. https://doi.org/10.1039/b816424j PMID: 19225618

28. Pereira F, Duarte-Pereira S, Silva RM, da Costa LT, Pereira-Castro I. Evolution of the NET (NocA, Nlz, Elbow, TLP-1) protein family in metazoans: insights from expression data and phylogenetic analysis. Scientific reports. 2016; 6:38383. https://doi.org/10.1038/srep38383 PMID: 27929068

29. Nien C-Y, Liang H-L, Butcher S, Sun Y, Fu S, Gocha T, et al. Temporal coordination of gene networks by Zelda in the early Drosophila embryo. PLoS Genetics. 2011; 7(10):e1002339. https://doi.org/10.1371/journal.pgen.1002339 PMID: 22028675

30. Biedler JK, Hu W, Tae H, Tu Z. Identification of early zygotic genes in the yellow fever mosquito Aedes aegypti and discovery of a motif involved in early zygotic genome activation. Plos One. 2012; 7(3):e33933. https://doi.org/10.1371/journal.pone.0033933 PMID: 22457801

31. Brown P, Baxter L, Hickman R, Beynon J, Moore JD, Ott S. MEME-LaB: motif analysis in clusters. Bioinformatics. 2013; 29(13):1696–7. https://doi.org/10.1093/bioinformatics/btt248 PMID: 23681125

32. Huang DW, Sherman BT, Lempicki RA. Systematic and integrative analysis of large gene lists using DAVID bioinformatics resources. Nature Protocols. 2009; 4(1):44–57. https://doi.org/10.1038/nprot.2008.211 PMID: 19131956

33. Nestorov P, Battke F, Levesque MP, Gerberding M. The maternal transcriptome of the crustacean Parhyale hawaiensis is inherited asymmetrically to invariant cell lineages of the ectoderm and mesoderm. Plos One. 2013; 8(2):e56049. https://doi.org/10.1371/journal.pone.0056049 PMID: 23418507

34. Wang J, Garrey J, Davis RE. Transcription in pronuclei and one- to four-cell embryos drives early development in a nematode. Current Biology. 2014; 24(2):124–33. https://doi.org/10.1016/j.cub.2013.11.045 PMID: 24374308

35. El-Sherif E, Averof M, Brown SJ. A segmentation clock operating in blastoderm and germband stages of Tribolium development. Development. 2012; 139(23):4341–6. https://doi.org/10.1242/dev.085126 PMID: 23095886

36. van der Zee M, Berns N, Roth S. Distinct functions of the Tribolium zerknüllt genes in serosa specification and dorsal closure. Current Biology. 2005; 15(7):624–36. https://doi.org/10.1016/j.cub.2005.02.057 PMID: 15823534

37. Savard J, Marques-Souza H, Aranda M, Tautz D. A segmentation gene in tribolium produces a polycistronic mRNA that codes for multiple conserved peptides. Cell. 2006; 126(3):559–69. https://doi.org/10.1016/j.cell.2006.05.053 PMID: 16901788

38. Nunes da Fonseca R, von Levetzow C, Kalscheuer P, Basal A, van der Zee M, Roth S. Self-regulatory circuits in dorsoventral axis formation of the short-germ beetle Tribolium castaneum. Developmental Cell. 2008; 14(4):605–15. https://doi.org/10.1016/j.devcel.2008.02.011 PMID: 18410735

39. Chen G, Handel K, Roth S. The maternal NF-kappaB/dorsal gradient of Tribolium castaneum: dynamics of early dorsoventral patterning in a short-germ beetle. Development. 2000; 127(23):5145–56. PMID: 11060240

40. Choe CP, Miller SC, Brown SJ. A pair-rule gene circuit defines segments sequentially in the short-germ insect Tribolium castaneum. Proceedings of the National Academy of Sciences of the United States of America. 2006; 103(17):6560–4. https://doi.org/10.1073/pnas.0510440103 PMID: 16611732

41. Nakamoto A, Hester SD, Constantinou SJ, Blaine WG, Tewksbury AB, Matei MT, et al. Changing cell behaviours during beetle embryogenesis correlates with slowing of segmentation. Nature Communications. 2015; 6:6635. https://doi.org/10.1038/ncomms7635 PMID: 25858515

42. Paré AC, Vichas A, Fincher CT, Mirman Z, Farrell DL, Mainieri A, et al. A positional Toll receptor code directs convergent extension in Drosophila. Nature. 2014; 515(7528):523–7. https://doi.org/10.1038/nature13953 PMID: 25363762

43. Benton MA, Pechmann M, Frey N, Stappert D, Conrads KH, Chen Y-T, et al. Toll genes have an ancestral role in axis elongation. Current Biology. 2016; 26(12):1609–15. https://doi.org/10.1016/j.cub.2016.04.055 PMID: 27212406

44. Brown SJ, Mahaffey JP, Lorenzen MD, Denell RE, Mahaffey JW. Using RNAi to investigate orthologous homeotic gene function during development of distantly related insects. Evolution & Development. 1999; 1(1):11–5.

45. Lavore A, Pagola L, Esponda-Behrens N, Rivera-Pomar R. The gap gene giant of Rhodnius prolixus is maternally expressed and required for proper head and abdomen formation. Developmental Biology. 2012; 361(1):147–55. https://doi.org/10.1016/j.ydbio.2011.06.038 PMID: 21763688

46. Berni M, Fontenele MR, Tobias-Santos V, Caceres-Rodrigues A, Mury FB, Vionette-do-Amaral R, et al. Toll signals regulate dorsal-ventral patterning and anterior-posterior placement of the embryo in the hemipteran Rhodnius prolixus. EvoDevo. 2014; 5:38. https://doi.org/10.1186/2041-9139-5-38 PMID: 25908955

47. Pires CV, Freitas FCdP, Cristino AS, Dearden PK, Simões ZLP. Transcriptome Analysis of Honeybee (Apis Mellifera) Haploid and Diploid Embryos Reveals Early Zygotic Transcription during Cleavage. Plos One. 2016; 11(1):e0146447. https://doi.org/10.1371/journal.pone.0146447 PMID: 26751956

48. Arsala D, Lynch JA. Ploidy has little effect on timing early embryonic events in the haplo-diploid wasp Nasonia. Genesis. 2017; 55(5). https://doi.org/10.1002/dvg.23029 PMID: 28432826;

49. Tomoyasu Y, Wheeler SR, Denell RE. Ultrabithorax is required for membranous wing identity in the beetle Tribolium castaneum. Nature. 2005; 433(7026):643–7. https://doi.org/10.1038/nature03272 PMID: 15703749

50. Tomoyasu Y, Denell RE. Larval RNAi in Tribolium (Coleoptera) for analyzing adult development. Development Genes and Evolution. 2004; 214(11):575–8. https://doi.org/10.1007/s00427-004-0434-0 PMID: 15365833

51. Tomoyasu Y, Arakane Y, Kramer KJ, Denell RE. Repeated co-options of exoskeleton formation during wing-to-elytron evolution in beetles. Current Biology. 2009; 19(24):2057–65. https://doi.org/10.1016/j.cub.2009.11.014 PMID: 20005109

52. Ravisankar P, Lai Y-T, Sambrani N, Tomoyasu Y. Comparative developmental analysis of Drosophila and Tribolium reveals conserved and diverged roles of abrupt in insect wing evolution. Developmental Biology. 2016; 409(2):518–29. https://doi.org/10.1016/j.ydbio.2015.12.006 PMID: 26687509

53. Panganiban G, Nagy L, Carroll SB. The role of the Distal-less gene in the development and evolution of insect limbs. Current Biology. 1994; 4(8):671–5. PMID: 7953552

54. Beermann A, Jay DG, Beeman RW, Hülskamp M, Tautz D, Jürgens G. The Short antennae gene of Tribolium is required for limb development and encodes the orthologue of the Drosophila Distal-less protein. Development. 2001; 128(2):287–97. PMID: 11124123

55. Angelini DR, Kikuchi M, Jockusch EL. Genetic patterning in the adult capitate antenna of the beetle Tribolium castaneum. Developmental Biology. 2009; 327(1):240–51. https://doi.org/10.1016/j.ydbio.2008.10.047 PMID: 19059230

56. Angelini DR, Kaufman TC. Insect appendages and comparative ontogenetics. Developmental Biology. 2005; 286(1):57–77. https://doi.org/10.1016/j.ydbio.2005.07.006 PMID: 16112665

57. Boxshall GA. The evolution of arthropod limbs. Biological Reviews of the Cambridge Philosophical Society. 2004; 79(2):253–300. PMID: 15191225

58. Angelini DR, Smith FW, Jockusch EL. Extent With Modification: Leg Patterning in the Beetle Tribolium castaneum and the Evolution of Serial Homologs. G3 (Bethesda, Md). 2012; 2(2):235–48. https://doi.org/10.1534/g3.111.001537 PMID: 22384402

59. Suzuki Y, Squires DC, Riddiford LM. Larval leg integrity is maintained by Distal-less and is required for proper timing of metamorphosis in the flour beetle, Tribolium castaneum. Developmental Biology. 2009; 326(1):60–7. https://doi.org/10.1016/j.ydbio.2008.10.022 PMID: 19022238

60. Hug CB, Grimaldi AG, Kruse K, Vaquerizas JM. Chromatin Architecture Emerges during Zygotic Genome Activation Independent of Transcription. Cell. 2017; 169(2):216–28 e19. https://doi.org/10.1016/j.cell.2017.03.024 PMID: 28388407.

61. Li X-Y, Harrison MM, Villalta JE, Kaplan T, Eisen MB. Establishment of regions of genomic activity during the Drosophila maternal to zygotic transition. eLife. 2014; 3. https://doi.org/10.7554/eLife.03737 PMID: 25313869

62. Xu Z, Chen H, Ling J, Yu D, Struffi P, Small S. Impacts of the ubiquitous factor Zelda on Bicoid-dependent DNA binding and transcription in Drosophila. Genes & Development. 2014; 28(6):608–21. https://doi.org/10.1101/gad.234534.113 PMID: 24637116

63. Foo SM, Sun Y, Lim B, Ziukaite R, O'Brien K, Nien C-Y, et al. Zelda potentiates morphogen activity by increasing chromatin accessibility. Current Biology. 2014; 24(12):1341–6. https://doi.org/10.1016/j.cub.2014.04.032 PMID: 24909324

64. Schulz KN, Bondra ER, Moshe A, Villalta JE, Lieb JD, Kaplan T, et al. Zelda is differentially required for chromatin accessibility, transcription factor binding, and gene expression in the early Drosophila embryo. Genome Res. 2015; 25(11):1715–26. https://doi.org/10.1101/gr.192682.115 PMID: 26335634;

65. Sun Y, Nien CY, Chen K, Liu HY, Johnston J, Zeitlinger J, et al. Zelda overcomes the high intrinsic nucleosome barrier at enhancers during Drosophila zygotic genome activation. Genome Res. 2015; 25(11):1703–14. https://doi.org/10.1101/gr.192542.115 PMID: 26335633;

66. Jacobs CG, Rezende GL, Lamers GE, van der Zee M. The extraembryonic serosa protects the insect egg against desiccation. Proc Biol Sci. 2013; 280(1764):20131082. https://doi.org/10.1098/rspb.2013.1082 PMID: 23782888;

67. Nicholson DB, Ross AJ, Mayhew PJ. Fossil evidence for key innovations in the evolution of insect diversity. Proc Biol Sci. 2014; 281(1793). Epub 2014/08/29. https://doi.org/10.1098/rspb.2014.1823 PMID: 25165766;

68. Altschul SF, Madden TL, Schaffer AA, Zhang J, Zhang Z, Miller W, et al. Gapped BLAST and PSI-BLAST: a new generation of protein database search programs. Nucleic Acids Res. 1997; 25(17):3389–402. PMID: 9254694;

69. Finn RD, Coggill P, Eberhardt RY, Eddy SR, Mistry J, Mitchell AL, et al. The Pfam protein families database: towards a more sustainable future. Nucleic Acids Research. 2016; 44(D1):D279–85. https://doi.org/10.1093/nar/gkv1344 PMID: 26673716

70. Clark K, Karsch-Mizrachi I, Lipman DJ, Ostell J, Sayers EW. GenBank. Nucleic Acids Res. 2016; 44(D1):D67–72. https://doi.org/10.1093/nar/gkv1276 PMID: 26590407;

71. Giraldo-Calderon GI, Emrich SJ, MacCallum RM, Maslen G, Dialynas E, Topalis P, et al. VectorBase: an updated bioinformatics resource for invertebrate vectors and other organisms related with human diseases. Nucleic Acids Res. 2015; 43(Database issue):D707–13. https://doi.org/10.1093/nar/gku1117 PMID: 25510499;

72. Bailey TL. DREME: motif discovery in transcription factor ChIP-seq data. Bioinformatics. 2011; 27(12):1653–9. https://doi.org/10.1093/bioinformatics/btr261 PMID: 21543442

73. Bailey TL, Boden M, Buske FA, Frith M, Grant CE, Clementi L, et al. MEME SUITE: tools for motif discovery and searching. Nucleic Acids Research. 2009; 37(Web Server issue):W202–8. https://doi.org/10.1093/nar/gkp335 PMID: 19458158

74. Zhu LJ, Christensen RG, Kazemian M, Hull CJ, Enuameh MS, Basciotta MD, et al. FlyFactorSurvey: a database of Drosophila transcription factor binding specificities determined using the bacterial one-hybrid system. Nucleic Acids Res. 2011; 39(Database issue):D111–7. https://doi.org/10.1093/nar/gkq858 PMID: 21097781;

75. Gupta S, Stamatoyannopoulos JA, Bailey TL, Noble WS. Quantifying similarity between motifs. Genome Biology. 2007; 8(2):R24. https://doi.org/10.1186/gb-2007-8-2-r24 PMID: 17324271

76. Grant CE, Bailey TL, Noble WS. FIMO: scanning for occurrences of a given motif. Bioinformatics. 2011; 27(7):1017–8. https://doi.org/10.1093/bioinformatics/btr064 PMID: 21330290

77. Kinsella RJ, Kähäri A, Haider S, Zamora J, Proctor G, Spudich G, et al. Ensembl BioMarts: a hub for data retrieval across taxonomic space. Database: the Journal of Biological Databases and Curation. 2011; 2011:bar030. https://doi.org/10.1093/database/bar030 PMID: 21785142

78. Lord JC, Hartzer K, Toutges M, Oppert B. Evaluation of quantitative PCR reference genes for gene expression studies in Tribolium castaneum after fungal challenge. Journal of Microbiological Methods. 2010; 80(2):219–21. https://doi.org/10.1016/j.mimet.2009.12.007 PMID: 20026205

79. Misof B, Liu S, Meusemann K, Peters RS, Donath A, Mayer C, et al. Phylogenomics resolves the timing and pattern of insect evolution. Science. 2014; 346(6210):763–7. https://doi.org/10.1126/science.1257570 PMID: 25378627

80. Minakuchi C, Namiki T, Shinoda T. Krüppel homolog 1, an early juvenile hormone-response gene downstream of Methoprene-tolerant, mediates its anti-metamorphic action in the red flour beetle Tribolium castaneum. Developmental Biology. 2009; 325(2):341–50. https://doi.org/10.1016/j.ydbio.2008.10.016 PMID: 19013451

81. Lynch JA, Peel AD, Drechsler A, Averof M, Roth S. EGF signaling and the origin of axial polarity among the insects. Current Biology. 2010; 20(11):1042–7. https://doi.org/10.1016/j.cub.2010.04.023 PMID: 20471269